

Source: Simmons 2002 [157578], SN-LBNL-SCI-108-V2, p. 6.

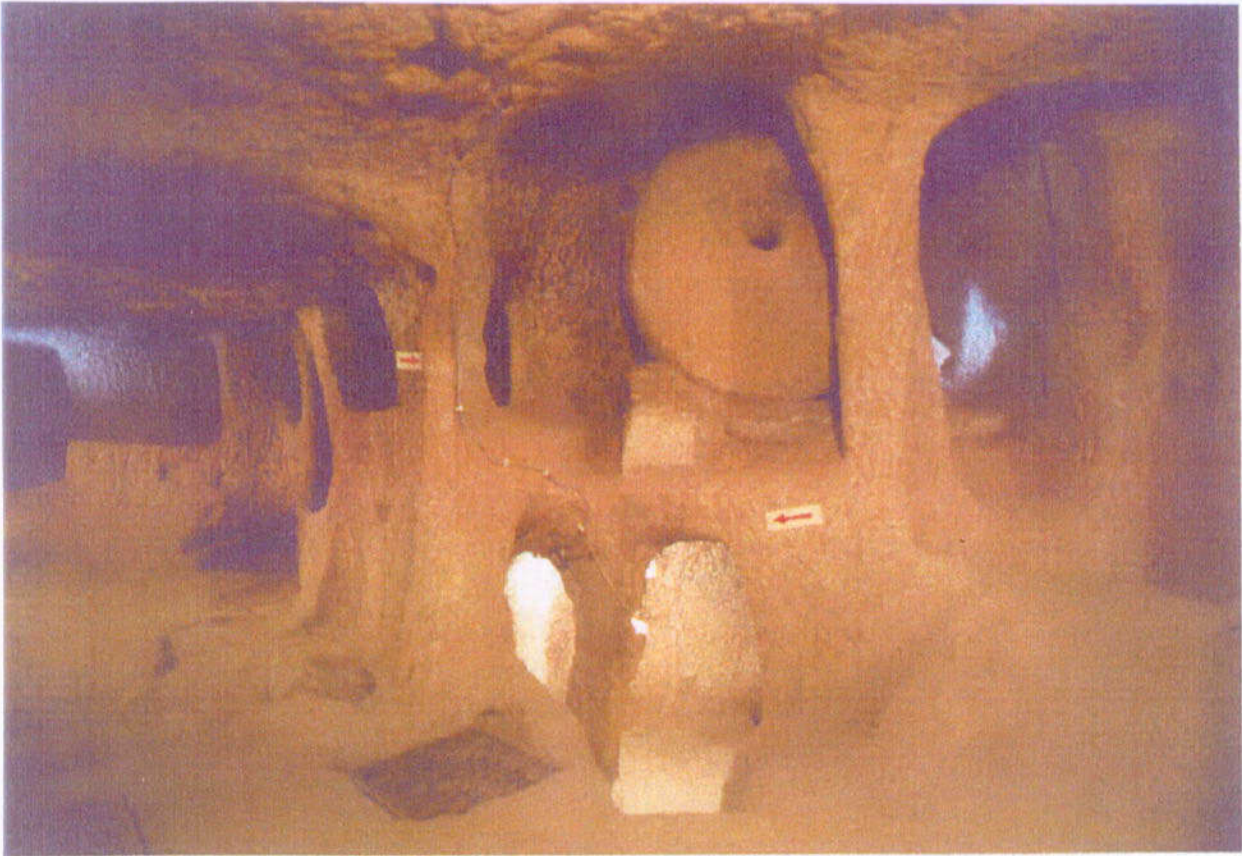
Figure 3-3. Photographs of the Nubian Limestone That Hosts the Tombs in the Valley of the Kings, Egypt



NOTE: The roof is formed by mica schist and the floor by marble. Ground support appears to be modern because older reports make no mention of either wood or cement.

Source: Gill 2001 [157516].

Figure 3-4. Mined Out Cavern in the Laurion Mines, Greece



NOTE: The millstone is about 1.5 m in diameter.

Source: Stuckless 2000 [151957], Figure 13.

Figure 3-5. Photograph of a Room in the Underground City of Kaymakli, Turkey

4. ANALOGUES TO WASTE FORM DEGRADATION

4.1 INTRODUCTION

Many variations of waste form types may be emplaced within a potential repository at Yucca Mountain. However, most of the waste will be spent fuel in the form of UO_2 , with the remaining 10% or so being encapsulated in borosilicate glass resulting from vitrification of defense high-level nuclear waste. These waste forms are thermodynamically unstable under wet, oxidizing conditions (DOE 2001 [153849], 4.2.6.1). For this reason, quantification of the degradation modes and dissolution rates that determine the source term for performance assessment is extremely important.

Analogue studies may contribute to understanding long-term waste form degradation processes through the record left behind in secondary minerals and groundwater. Many of the published analogue studies of waste form degradation focus on dissolution of uranium under reducing groundwater conditions. This is because most of the geologic waste disposal configurations of other nations involve saturated, reducing conditions. Sketches of the most important and well-studied of these analogue sites were provided in Section 13 of the *Yucca Mountain Site Description* (CRWMS M&O 2000 [151945]). As a whole, the sites with reducing groundwater chemistry have limited applicability to conditions that would be expected to occur at a potential Yucca Mountain repository, which is located in an unsaturated oxidizing environment. However, in some instances, information from these analogue studies can still provide valuable insights into the processes of waste form degradation. Section 4 relies to the extent possible on information derived from oxidizing environments, but relevant information from examples in reducing environments is included to illustrate general principles of waste form dissolution and potential criticality.

Section 4.2 provides a conceptual basis for waste form degradation. Section 4.3 discusses analogues relevant to spent-fuel dissolution rates. Section 4.4 addresses the formation of secondary minerals that may immobilize uranium and fission products. Section 4.5 briefly covers radiolysis and Section 4.6 briefly covers nuclear criticality of the waste form. Section 4.7 summarizes studies of analogues to glass waste forms. Section 4.8 is a summary of the topics discussed.

4.2 WASTE FORM DEGRADATION—CONCEPTUAL BASIS

4.2.1 Overview of Conceptual Basis

Radionuclide release from the waste forms that would be emplaced at Yucca Mountain is a three-step process requiring: (1) degradation of the waste forms, (2) mobilization of the radionuclides from the degraded waste forms, and (3) transport of the radionuclides away from the waste forms (DOE 2001 [153849], 4.2.6.1). Water strongly influences all three processes.

As described in the S&ER (DOE 2001 [153849], 4.2.6.1) radionuclide release begins after breach of the waste package and the ingress of air. If the breach is early, the waste may still be

highly radioactive and physically hot. The thermal output of hot waste packages, particularly from commercial spent fuel, will limit groundwater access at early times. When water enters the package, the rate of water inflow and evaporation will determine when and if water accumulates. During this period, gamma radiolysis (radiation-induced decomposition) of the humid air within the package may cause production of nitric acid, which could condense into any accumulated water. If the breach is late, radiation levels and heat will be much lower, and evaporation and radiolytic acid production will be less important. During either period, water may enter the package either as water vapor or as liquid. The dissolved constituents in the groundwater entering the package may have a significant effect on in-package chemistry only if evaporation has concentrated them by orders of magnitude. This is unlikely to occur unless the waste package is breached only at the top and large amounts of water enter and evaporate within the package. During the latter period, there is no water transport of groundwater species or radionuclides out of the package.

If the package overflows, or if holes in the bottom allow flow-through, fresh water will dilute the groundwater components, and water-based radionuclide releases may begin. The release of radionuclides does not begin until after the breach of the cladding (for spent fuel). Chemistry within the package is important because it influences the rate of degradation of the package and waste forms (including cladding), and it determines the mobility of radionuclides as dissolved or colloidal species. Films of stagnant, concentrated, acidified groundwater are considered the worst possible scenario for degradation, because they do not inhibit oxygen and carbon dioxide transport and may support localized corrosion of the cladding and waste. Such films, however, do not support significant mobilization and transport of radionuclides and are only possible at times when there is an exact balance of water inflow and evaporation.

As stated previously, most of the many waste form types that may be emplaced within a repository are thermodynamically unstable under wet, oxidizing conditions (DOE 2001 [153849], 4.2.6.1). Uranium dioxide fuels will oxidize and hydrate, and glass waste forms will react with water to form clays, zeolites, and oxides. The rate of these reactions, however, will in most cases be quite slow and may be limited by the rate that reactants such as oxygen and water can be transported to the waste form surface. Although a few radionuclides such as cesium and iodine may concentrate between the fuel and cladding during reactor operation, most of the radionuclides will be incorporated within the various waste forms and cannot be released from the waste package until the waste forms degrade.

Once the waste forms degrade, radionuclides as dissolved species and suspended particles may be mobilized by advection or diffusion. Larger particles settle out of solution, or are filtered out by trapping in small openings. Only after gross failure of the package will these larger particles fall or wash out of the package. Particles in the colloid size range, however, can remain suspended and may travel significant distances. The concentration of radionuclides associated with colloids is limited by the colloid concentration and radionuclide carrying capacity of the colloids (DOE 2001 [153849], Section 4.2.6.1). The concentration of dissolved species is limited by the elemental solubility of the radionuclide within the local environment.

4.2.2 Spent Fuel Dissolution in an Oxidizing Environment

Many laboratory studies attempt to measure parameters that can be used to determine the rate of spent fuel dissolution under repository disposal conditions. These studies use either spent fuel itself, uranium dioxide (as an analogue for spent fuel), or uraninite as a natural analogue. Although the uraninite structure can accommodate some degree of oxidation, in highly oxidizing aqueous environments uraninite is unstable and decomposes (Finch and Ewing 1992 [113030], p. 133). Secondary uranyl (U^{+6})-bearing phases precipitate on the surface of the corroding uraninite, and a rind of corrosion products forms. The impurities often contained in uraninite affect its thermodynamic properties, the rate of uraninite alteration, and the composition of the corrosion products (Finch and Ewing 1991 [105591], p. 392). Studies that have examined the dissolution of uraninites under oxidizing conditions found that the dissolution rate was diminished by the presence of thorium, lead, and rare-earth-element impurities in the uraninite (Finch and Ewing 1992 [113030], p. 133). Compared to uraninite, spent fuel has a lower content of these impurities (Finch and Ewing 1992 [127908], p. 466) and on this basis might be considered to dissolve more rapidly.

Most of the uranium released to solution during the dissolution of UO_2 combines with ions in water to form secondary alteration phases. Both natural and experimental uranium systems display a paragenetic sequence of mineral phase formation that is characterized by the following general trend (Stout and Leider 1997 [100419], Section 2.1.3.5):

$UO_2 \Rightarrow$ uranyl oxide hydrates \Rightarrow alkali and alkaline-earth uranyl oxide hydrates \Rightarrow
uranyl silicates \Rightarrow alkali- and alkaline earth uranyl silicates + palygorskite clay.

Specifically, mineralization in the experimentally determined paragenetic sequence of alteration phases is:

$UO_2 \Rightarrow$ dehydrated schoepite ($UO_3 \cdot 2H_2O$) \Rightarrow compreignacite $K_2(UO_2)_6O_4(OH)_6 \cdot 8H_2O$
+ becquerelite ($Ca(UO_2)_6O_4(OH)_6 \cdot 8H_2O$) \Rightarrow soddyite ($(UO_2)_2SiO_4 \cdot 2H_2O$) \Rightarrow
boltwoodite ($K(H_3O)(UO_2)SiO_4$) + uranophane ($Ca(UO_2)_2Si_2O_7 \cdot 6H_2O$) + palygorskite
clay (Wronkiewicz et al. 1996 [102047], p. 94).

Thus, the uranyl oxide hydrates are common initial corrosion products of uraninite during weathering. In the presence of dissolved silica, these early phases alter to uranyl silicates, most commonly soddyite and uranophane. The phases that form depend on the chemical composition of the waters with which the uraninite is in contact, which in turn depends on the mineralogy of the surrounding host rocks and the oxidation potential of the hydrologic environment. The experimentally determined mineral sequence appears to be controlled by precipitation kinetics and is nearly identical to secondary uranium phases observed during the weathering of naturally occurring uraninite under oxidizing conditions, such as that which occurs at the Nopal I uranium deposit, Peña Blanca, Mexico (Wronkiewicz et al. 1996 [102047], Figure 7). In laboratory UO_2 tests and in the natural uranium deposits at Nopal I, the alkali- and alkaline-earth uranyl silicates represent the long-term solubility-limiting phases for uranium (Stout and Leider 1997 [100419], Section 2.1.3.5). Furthermore, at Nopal I, uranium concentrations in groundwater and seepage waters ranged from 170 parts per trillion (ppt) to 6 parts per billion (ppb) (Pickett and Murphy 1999 [110009], Table 2). The upper part of this range is similar to concentrations seen in filtered

samples from spent fuel dissolution experiments (Stout and Leider 1997 [100419], p. 2.1.3.5-4). This added similarity increases confidence that the experiments and the natural analogue reactions may simulate the long-term reaction progress of spent UO₂ fuel following potential disposal at Yucca Mountain.

Uraninite usually contains radiogenic lead that has in-grown through time (Finch and Ewing 1992 [127908], p. 466). As a result, the early-formed Pb-poor uranyl oxide hydrates alter incongruently to uranyl silicates plus radiogenic-Pb-enriched uranyl oxide hydrates, such as curite (Pb₂U₅O₁₇ · 4H₂O), that may serve to limit the mobility of uranium in nature (Finch and Ewing 1992 [127908], p. 466). Curite may also play an important role in the formation of uranyl phosphates, which are significantly less soluble than the uranyl silicates and control uranium solubility in many groundwaters associated with altered uranium ore (Finch and Ewing 1992 [127908], p. 465). In the absence of lead, schoepite and becquerelite are the common initial corrosion products. The reaction path for the alteration of lead-free uraninite results in the formation of uranyl silicates. Thus, the long-term oxidation behavior for ancient, lead-bearing uraninite is different from that of young, lead-free uraninite, which is more similar to spent fuel. Because the presence of lead effectively reduces the mobility of uranium in oxidizing waters, the concentration of uranium in groundwaters associated with oxidized uranium ore deposits will depend in part on the age of the primary uraninite (Finch and Ewing 1992 [113030], p. 133).

In summary, the paragenesis of uraninite alteration phases depends on the age of the primary uraninite, the mineralogy of surrounding host rocks, and on groundwater composition, pH, and redox potential. In a general oversimplification, the progression of phases of uraninite alteration, in the absence of radiogenic lead in-growth, will be to uranyl silicates, culminating in uranophane in an oxidizing environment. Numerous compositional variations are caused by trace elements present in the system. The composition of schoepite is often used to represent an alteration product in models of spent fuel alteration, but this is an oversimplification, based on observations in nature. As shown by Finch and Ewing (1992 [113030], p. 144), the formation of intermediate-phase schoepite may be favored early during the corrosion of uraninite. Schoepite is not, however, a long-term solubility-limiting phase for oxidized uranium in natural groundwaters containing dissolved silica or carbonate (e.g., the type of groundwaters at Yucca Mountain).

Despite the analogy between uraninite and spent fuel, there are important differences between the two. For one thing, spent fuel is artificially enriched in ²³⁵U and contains nuclear fission products that are not present in uraninite; in contrast, uraninite contains a higher proportion of nonradiogenic trace element impurities. Also, the thermal history of spent fuel, unlike that of natural uraninite, may cause lattice and structural crystallization defects in the spent fuel that are not present in the uraninite. In addition, geologically old uraninite contains in-grown radiogenic lead, which would not be found in younger uraninite or in spent fuel. Section 4.3 presents the general dissolution path of uraninite, and by analogy spent fuel, under oxidizing conditions.

4.3 ANALOGUE STUDIES RELATED TO WASTE FORM DISSOLUTION RATES

The remaining issues of most relevance to the behavior of spent fuel in a repository that could be addressed by natural analogues are dissolution and radionuclide release (Section 4.3),

radionuclide retardation by secondary alteration products (Section 4.4), radiolysis (Section 4.5), and criticality (Section 4.6).

4.3.1 Fission-Product Tracer Method

Rates of UO_2 dissolution can be quantified by measuring the amount of fission product released from the uraninite and using this as a tracer. Concentrations of this tracer in the rock or in the groundwater in the vicinity of the uraninite are proportional to the dissolution rate, assuming that the tracer is released from the uraninite only by dissolution (Curtis 1996 [157497]; Curtis et al. 1994 [105270]; 1999 [110987]). The tracers used for this method are ^{99}Tc in rock, or its stable daughter ^{99}Ru , when technetium has decayed to insignificant amounts, and ^{129}I in groundwater. There are several uncertainties in the modeling and assumptions made in this approach, but some consistency is apparent in the results obtained from different uranium orebodies when using the same isotopic system. For example, using the ^{99}Tc tracer at Oklo, Gabon, and at Cigar Lake, Canada, provided average release rates of 1.5×10^{-6} per year and 1.1×10^{-6} per year, respectively (Curtis 1996 [157497], p. 145). However, different rates are obtained when using ^{129}I as a tracer. Applying this tracer at Cigar Lake provided release rates of between 9×10^{-9} and 3×10^{-10} per year, which are 2 to 4 orders of magnitude less than the values obtained using the ^{99}Tc tracer.

Curtis et al. (1994 [105270]) used measurements of ^{99}Tc , ^{129}I , ^{239}Pu , and U concentrations in rock from uranium deposits at Cigar Lake and Koongarra to estimate radionuclide release rates from uranium minerals. At Koongarra, Australia, release rates appear to have been faster (10^{-7} per year; Curtis et al. 1994 [105270], p. 2234) than at Cigar Lake, where model-dependent release constants from the uraninite bearing rocks were $<5 \times 10^{-8}$ per year (Curtis et al. 1994 [105270], p. 2234), producing small deficiencies of ^{99}Tc , and larger ones of ^{129}I . The inferred differences in radionuclide release rates are consistent with expected differences in uranium mineral degradation rates produced by the differing hydrogeochemical environments at the two sites. In the Cigar Lake ore zone, low uraninite solubility in a reducing environment and small water flux through impermeable rock would inhibit the rate of uraninite degradation and thus the rate of radionuclide release. At Koongarra, higher mineral solubilities induced by higher oxidation potentials, higher aqueous concentrations of carbonate and phosphate, and greater water fluxes would be expected to produce higher rates of uranium mineral degradation. Curtis et al. (1999 [110987], p. 284) note that the consistency of $^{239}\text{Pu}/\text{U}$ and $^{99}\text{Tc}/\text{U}$ ratios in bulk rock suggests that the redistribution processes observed at Cigar Lake are highly localized and do not result in large-scale losses or gains of these nuclear products from the deposit as a whole. The fission product tracer method could be applied to water samples collected at Peña Blanca (Section 10.4). While this method clearly has potential for quantifying UO_2 dissolution under natural conditions, the method has yet to be refined and differences between results for the two tracers explained. Besides this fission product tracer method, there is no other technique for quantifying directly long-term uraninite dissolution rates in natural analogue studies.

4.3.2 Dissolution of Oklo Uraninite

Application of the fission-product tracer method has not been reported for Oklo, but Oklo provides a unique record of uranium and fission-product retention. Because parts of the Oklo orebody achieved nuclear criticality as a result of highly enriched concentrations of ^{235}U , Oklo

uraninite contains significant quantities of fission products or their stable daughters, directly equivalent to those present in spent fuel. In this regard, Oklo is unlike any other known uranium deposit. A photograph of one of the reactor zones is shown in Figure 4-1.

There are, however, some differences between Oklo uraninite and spent fuel. For one thing, Oklo contains lower concentrations of fission products than does spent fuel. Also the temperature of reaction (400° to 600°C; for a discussion of temperatures, see Zetterström 2000 ([157501], p. 13) and power density were somewhat lower than in a reactor, and the duration of criticality at Oklo (on the order of 0.1 to 0.8 Ma; Louvat and Davies 1998 [125914], p. 140) was much longer than the lifetime of reactor fuel. Recognizing these differences, several large-scale analogue investigations have taken place at Oklo, and much relevant information has been obtained, including semiquantitative information on the fate of radionuclides contained in the orebody.

These analogue investigations (e.g., Louvat and Davies 1998 [125914]; Gauthier-Lafaye et al. 2000 [157499]) have revealed that when the Oklo reactor zones were cooling after periods of criticality, some dissolution of the uraninite and elemental remobilization occurred. However, the limited extent of this remobilization is indicated by the fact that more than 90% of the uranium "fuel" has remained in the same spatial configuration since criticality (Miller et al. 2000 [156684], p. 81). This implies that uranium has been almost fully retained within the uraninite minerals. The disposition of some performance assessment-relevant elements and other elements in the reactor zones at Oklo is provided in Table 4-1. The transuranic elements neptunium, plutonium, and americium were all formed *in situ* within the uraninite during criticality, and their stable daughters have also been retained due to their compatibility with the crystal chemical structure of their host or in inclusions in the uraninite. Other radiogenic elements, which were less compatible with the uraninite host (e.g., Cs, Rb, Sr, Ba) have been partially or totally lost by diffusion from the uraninite. Some elements (e.g., Tc, Ru, Rh, Pd), however, migrated only short distances and were totally retained within the clay matrix enclosing the reactors. Data for other elements indicate clear deficiencies in the noble gases, halides, and lead (possibly resulting from volatilization) and suggest that some minor loss from the system has occurred for other elements.

Because the reactions ended nearly two billion years ago, the short-lived radionuclides have decayed to more stable daughter nuclides. Analysis of the behavior of these short-lived radionuclides is problematic. According to Brookins (1978 [133930], p. 309), Pu, Np, and Am were likely retained within the reactor, while Bi and Pb would have been redistributed locally without substantial migration (Brookins 1978 [133930], p. 309). Most geochemical observations at Oklo support these predictions to varying degrees. Curtis et al. (1989 [100438], p. 57) conclude that the retention of fission products is related to their partitioning into uraninite or secondary mineral assemblages. Those fission products that partitioned into the secondary mineral assemblages were largely lost over time, pointing to the importance of small uraninite grains in controlling the chemical microenvironment.

It is important to note that most of the observed uraninite alteration at Oklo occurred under hydrothermal conditions. Little uraninite-groundwater interaction has taken place at present-day ambient temperatures, except at the shallow Bangombé reactor zone (Smellie et al. 1993 [126645], p. 144). In summary, the Oklo natural analogue investigations indicate that the kinetics of UO₂ dissolution, either as uraninite or spent fuel, are exceedingly low under reducing conditions expected in the near field of some repositories. While dissolution rates cannot be

quantified readily from natural analogue data, the abundance of naturally occurring uraninite that is nearly 2 billion years old at Oklo indicates its stability in the natural environment.

4.4 ANALOGUE STUDIES RELATED TO IMMOBILIZATION BY SECONDARY MINERALS

Laboratory experiments have shown that UO_2 dissolution is accompanied by the formation of secondary phases on the fuel surface and that these corrosion products can passivate further dissolution (Wronkiewicz et al. 1996 [102047], p. 79). At the temperature and time scales of laboratory experiments, these phases are amorphous. However, natural sites where uraninite accumulations occur and where dissolution has taken place over long time periods could provide insights into the structure and mineralogy of the secondary passivating phases, and indicate whether they have been able to prevent further mobilization of radionuclides.

4.4.1 Shinkolobwe, Zaire

The 1,800 Ma Shinkolobwe uranium orebody in Zaire (at the time of study) was the subject of a comprehensive investigation regarding the corrosion products of uraninite (Finch and Ewing 1991 [105591]). The Shinkolobwe deposit weathers under oxidizing conditions in a monsoonal-type environment where rainfall is above 1 m per year, thus providing more aggressive hydrochemical conditions than might be expected at a repository. At Shinkolobwe, the uraninite is coarsely crystalline and lacks many of the impurities, such as thorium and rare earth elements, found in other uranium deposits. This lack of impurities led Finch and Ewing (1991 [105591], p. 391) to suggest that the thermodynamic stability of the Shinkolobwe uraninite might closely approximate spent fuel.

The deposit has been exposed at the surface since the Tertiary (< 60 million years), and extensive weathering has altered or replaced much of the original uraninite. Uranium (VI) mineralization occurs along fracture zones where meteoric waters have penetrated up to 80 m deep or more. Uraninite crystals at Shinkolobwe are commonly surrounded by dense rinds of alteration minerals, mostly uranyl oxyhydroxides, as well as uranyl silicates and rutherfordine, a uranyl carbonate (UO_2CO_3). Uranyl phosphates are also common within fractures throughout the host rocks, but are rare or absent from corrosion rinds.

Uranyl minerals comprising the corrosion rinds that surround many uraninite crystals undergo continuous alteration. This alteration occurs through repeated interaction with carbonate- and Si-bearing groundwater combined with periodic dehydration of (especially) schoepite and metaschoepite (Finch and Ewing 1991 [105591], p. 396). Such alteration occurs along small (approx. 0.1 to 1 mm) veins within the corrosion rinds. There is a general decrease in grain size as alteration proceeds, most commonly along veins. Schoepite, however, is not observed to re-precipitate where in contact with dehydrated schoepite (Finch and Ewing 1991 [105591], p. 396). Thus, while the formation of schoepite early during the corrosion of uraninite may be favored, schoepite is not a long-term solubility-limiting phase for oxidized uranium in natural groundwaters containing dissolved silica or carbonate (e.g., the type of groundwaters at Yucca Mountain).

Over 50 secondary uranyl phases were identified from the alteration of the uraninite. It was concluded that uraninite transforms to Pb-U oxide hydrates and then to uranyl silicates if sufficient silica is present in the system. Alteration of Proterozoic (~2400 to 700 Ma) uranium deposits such as Shinkolobwe introduce the important Pb-bearing phases, such as curite, which play a role in development of other stable phases in the system. Because of the very young age of repository spent fuel, radiogenic lead would not be present at Yucca Mountain for helping to immobilize spent-fuel elements.

4.4.2 Secondary Phases of Uranium Found at Nopal I, Peña Blanca

See Section 10.4 for a description of the Nopal I site. At Nopal I, uraninite occurs in rhyolite tuff in a semi-arid environment, where it has been exposed to oxidizing groundwater conditions with nearly neutral pH. Uranium was initially deposited as uraninite at Nopal I approximately 8 Ma (Pearcy et al 1994 [100486], p. 729). Geologic, petrographic, and geochemical analyses indicate that primary uraninite at Nopal I has been almost entirely altered to hydrated oxides and silicates containing uranium in the oxidized (uranyl) form. Because of its young geologic age, the deposit is low in radiogenic lead. The sequence of formation of uranyl minerals by alteration of uraninite at Nopal I is shown in Figure 4-2 and is similar in many geologically young uranium deposits located in oxidizing environments.

Leslie et al. (1993 [101714]) and Pearcy et al. (1994 [100486]) compared the alteration of uraninite at Nopal I to laboratory experiments of degradation of spent nuclear fuel potentially to be disposed of at Yucca Mountain, Nevada. They found that uraninite from the Nopal I deposit should be a good natural analogue to spent nuclear fuel because long-term experiments on spent fuel show alteration parageneses, intergrowths, and morphologies that are very similar to those observed at Nopal I (Wronkiewicz et al. 1996 [102047]). Oxidation of the uraninite at Nopal I has produced an ordered suite of minerals, first forming schoepite, a uranyl oxyhydroxide, followed by hydrated uranyl silicates, such as soddyite (Figure 4-2). Consistent with a high calcium abundance in Nopal I groundwater, the dominant secondary uranium phase is uranophane, a hydrated calcium uranyl silicate. Because of the abundance of calcite at Yucca Mountain, uranophane would be a potential secondary phase there as well. In comparison, laboratory experiments find that the general trend is to form mixed uranium oxides, followed by uranyl oxyhydroxides, and finally uranium silicates, mostly uranophane with lesser amounts of soddyite (Wronkiewicz et al. 1996 [102047], p. 92). In addition, uraninite at Nopal I has a low trace-element component (average of 3 wt%) that compares well with that of spent nuclear fuel (typically < 5 wt% (Pearcy et al. 1994 [100486], p. 730)). The young age of the Nopal I deposit is another similarity to Yucca Mountain with respect to the absence of Pb-bearing secondary phases.

4.4.3 Secondary Phases at Okélobondo

In the first detailed study of the Okélobondo natural fission reactor in Gabon, which corresponds to the southern extension of the Oklo deposit (Figure 4-3), Jensen and Ewing (2001 [157500]) presented a history of uraninite alteration at that site showing complex mineralogical and textural relationships. The Okélobondo reactor is the deepest of the 16 natural reactors (Figure 4-3). It is situated at the base of a 2.5 m deep synform in the FA sandstone of the Francevillian Series. The Okélobondo reactor zone (RZOKE) developed at the interface between overlying brecciated

high-grade uranium-mineralized FA sandstone and underlying bitumen-rich black shale of the FB Formation. RZOKE is relatively small (2.7 m wide and > 4 m long) and contains a ~ 55 cm thick reactor core (Jensen and Ewing 2001 [157500], p. 32).

Criticality in RZOKE was facilitated by fixation and reduction of oxidized uranium by liquid bitumen and precipitation of uraninite into a dense microfracture network in the FA sandstone. The brecciation of the host rock may have been increased by overpressure created by the accumulation of hydrocarbon gases during diagenetic maturation of oil introduced into the FA sandstone. Chemical analyses and model estimates suggest that the ore grade at criticality at RZOKE was on the order of 20 wt% uranium. Operation of the reactor caused extensive dissolution of the FA sandstone and hydrothermal alteration of the black shale of the FB Formation. The sandstone dissolution was the major process that led to formation of the 2.5 m deep reactor synform and the high uranium concentrations (≤ 90 vol% uraninite) in the core of RZOKE (Jensen and Ewing 2001 [157500], p. 59).

The mineral assemblage of RZOKE is comparable to that reported in the other Oklo reactor zones, in that uraninite and Si-rich illite are the major phases in the reactor core, while chlorite and illite are the major phases in the so-called *argile de pile* (reactor clays forming a halo around the reactor zone). Galena (PbS) is also a major phase in the reactor zone. Minor coffinite (USiO₄) and (U,Zr) silicates were also observed in addition to several accessory phases: e.g., titanium oxides, La-bearing monazite, sulfides of Cu, Fe, Co, Ni, and Zn, and ruthenium arsenides. The minor and trace elements include Th, Zr, Al, P, Ce, and Nd that seldom exceed concentrations of 0.1 oxide wt% (Jensen and Ewing 2001 [157500], p. 59). Figure 4-4 shows galena, illite, and zircon embedded in a matrix of (U,Zr)-silicate in the center of the RZOKE reactor core.

The accessory (U,Zr)-silicate, phosphates, and ruthenium arsenides (\pm Pb, Co, Ni, and S) were of particular importance in secondary retardation of the fissiogenic isotopes (Jensen and Ewing 2001 [157500], p. 59). The (U,Zr)-silicate contains elevated concentrations of ZrO₂, ThO₂, Ce₂O₃, and Nd₂O₃ as compared with the "unaltered" uraninite. This result suggests that the fissiogenic ⁹⁰Sr, Zr, Ce, and Nd, as well as the Th precursors, were efficiently retarded by the (U,Zr)-silicate during their migration in the reactor zone. Lanthanide element fission products may also have been retained in rare La-bearing monazite observed in the *argile de pile* of RZOKE. Ruthenium arsenides incorporated fissiogenic Ru, probably including ⁹⁹Ru, the radiogenic daughter of ⁹⁹Tc.

The presence of lead-uranyl sulfate hydroxide hydrate, anglesite, partial dissolution of uraninite and galena, and the rapid oxidation of pyrite are evidence of a later shift toward oxidative alteration conditions in and around the reactor zone. Hence, the slightly oxidizing deep groundwaters at Okélobondo may have already reacted with the Okélobondo reactor zone.

4.5 RADIOLYSIS

Radiolysis is hydrolysis caused by radiation and results in production of charged species (hydrogen and hydroxide ions) that may react to form more mobile species. Radiolysis can affect both the waste form and the waste package. Because the waste canister is thinner than in previous designs (CRWMS M&O 1999 [107292], Table 5-4), it is not self-shielded, so radiation levels at the outside surface of the canister would be higher. However, it is not certain that

radiolysis will be a problem. The effects of radiolysis in the Oklo ore deposit were discussed by Curtis and Gancarz (1983 [124785]). They calculated the alpha- and beta-particle doses in the critical reaction zones during criticality and the energy provided to the fluid phase by these particles. This energy caused radiolysis of water and the production of reductants (H_2) and oxidants (O_2). The effect of these reductants and oxidants on the transport of radionuclides within and outside the reactors has been difficult to quantify. Iron is most reduced in the samples that show the greatest ^{235}U depletion. Curtis and Gancarz (1983 [124785], p. 36) suggested that the reduction of iron in the reactor zones and oxidation of U (IV) in uraninite was contemporaneous with the nuclear reactions and not a later supergene phenomenon of secondary enrichment. Curtis and Gancarz (1983 [124785], p. 36) suggested that radiolysis of water resulted in the reduction of Fe (III) in the reactor zones and the oxidation of uranium. Furthermore, the authors suggested that the oxidized uranium was transported out of the critical reaction zones and precipitated through reduction processes in the host rocks immediately outside the zones. The reduction processes likely involved organics or sulfides present in the host rocks. However, if the host rocks around the natural reactor cores had not contained species capable of reducing the oxidized uranium transported out of the cores, the uranium could have been transported much further from the critical reaction zones. The important point is that, even with intensive radiolysis, very little (only several percent) of the uranium in the natural reactors was mobilized (Naudet 1978 [126123], p. 590).

Jensen and Ewing (2001 [157500], p. 59) noted a migration of Ce from reactor core to rim at Okélobondo and suggested that this resulted from radiolysis taking place during reactor operation. Cerium, particularly, showed indication of redistribution in the reactor zone, when compared with Nd, in the uraninite rim. Because Ce^{3+} can be oxidized to Ce^{4+} , the difference in the behavior of Ce as compared with Nd, results from oxidative alteration. The different concentration of Ce in the uraninite rims, as compared with their cores across the reactor zone, was produced during reactor operation, perhaps as a result of radiolysis.

4.6 CRITICALITY

The uranium deposit at Oklo, which was the site of naturally occurring neutron-induced fission reactions over 2,000 Ma, was used as a basis for reviewing conditions and scenarios that might lead to nuclear criticality within and outside waste packages in the Swedish waste disposal configuration (Oversby 1996 [100485]). The Swedish concept involves disposal in deep granite with chemically reducing groundwaters, so the specific conditions are not relevant to those of oxidizing environments. Yet in either oxidizing or reducing conditions, the combination of simultaneous factors and probabilities required for criticality to occur seems very unlikely. For criticality to occur, sufficient ^{239}Pu and/or ^{235}U would need to accumulate together with enough water to allow for moderation of neutron energies. This would achieve a state where neutron-induced fission reactions could be sustained at a rate significantly above the natural rate of spontaneous fission. The chemical and physical conditions required to achieve nuclear criticality at Oklo were used by Oversby (1996 [100485]) to estimate the amounts of spent fuel uranium that would need to be assembled in a favorable geometry in order to produce a similar reactive situation in a geologic repository. The amounts of uranium that must be transported and redeposited to reach a critical configuration are extremely large in relation to those that could be transported under any reasonably achievable conditions, even under oxidizing conditions. In addition, transport and redeposition scenarios often require opposite chemical characteristics.

Oversby (1996 [100485], p. vii) concluded that the likelihood of achieving a critical condition caused by accumulation of a critical mass of uranium outside the canisters after disposal is nil, provided that space in the canisters is filled by low solubility materials that prevent entry of sufficient water to mobilize uranium. Criticality caused by plutonium outside the canister could be ruled out because it requires a series of processes, each of which has an increasingly small probability. Criticality caused by uranium outside the canister would require dissolution and transport of uranium under oxidizing conditions and deposition of uranium under reducing conditions. There is no credible mechanism to achieve both oxidizing and reducing conditions in the near-field repository host rock in the long term, after decay of the majority of alpha-active isotopes. Thus, the conditional probabilities required to achieve criticality caused by uranium make the likelihood that criticality would occur vanishingly low.

4.7 NUCLEAR WASTE GLASS ANALOGUES

Among the natural volcanic glasses, basalt glasses are compositionally the most similar to nuclear waste glasses (Lutze et al. 1987 [125923], p. 142). However, there are still substantial compositional differences. Basalt glass and nuclear waste glass are similar in silica content, alteration products, alteration layer morphologies, and alteration rates in laboratory experiments (Grambow et al. 1986 [119228]; Arai et al. 1989 [123814]; Cowan and Ewing 1989 [124396]). Basalt glass alteration has been studied in a number of environments including ocean-floor, subglacial, hydrothermal and surface conditions (Grambow et al. 1986 [119228]; Jercinovic et al. 1986 [125289]; Byers et al. 1987 [121857]; Jercinovic and Ewing 1987 [144605]; Arai et al. 1989 [123814]; Cowan and Ewing 1989 [124396]). Inferred alteration rates, as calculated from alteration rinds, range from 0.001 μm (micrometers)/1,000 years to 30 μm /1,000 years (Arai et al. 1989 [123814], p. 73).

Malow and Ewing (1981 [126058]) compared the thermal and chemical stabilities of two borosilicate glasses and one glass ceramic to those of three rhyolitic glasses through a variety of laboratory tests and observations of natural weathering. They concluded that natural glasses are much more stable than waste-form glasses as a result of higher silica contents in the natural glasses (74% versus 28 to 50% in waste-form glasses). Tektites (nonvolcanic glass of extraterrestrial or impact origin) range in age from $\sim 10^5$ years to 35 Ma and rarely show signs of alteration, dehydration, or devitrification (Lutze et al. 1987 [125923], p. 148). Their great durability may be a result of their high silica and alumina ($\sim 30\%$) contents and their low ($<4\%$) alkali contents (Lutze et al. 1987 [125923], p. 152).

The compositions of the glasses utilized in natural analogue studies differ somewhat from borosilicate glasses, and this makes a simple analogy dubious for quantitative purposes. High silica and alumina contents, along with low alkali contents and low water contents, are favorable for long-term preservation. The dissolution rates measured on natural glasses are variable, but always very slow. However, natural analogues cannot be used to provide a quantitative estimate for the time at which devitrification will begin, or the rate at which it will proceed in the repository environment. Natural glass studies do suggest that the rate of devitrification is too slow for the process to be significant in the repository. These studies have not, however, considered the effect of radiation. It might be possible to obtain relevant data on the radiation-induced effects on glass durability by examining glasses that contain uranium oxides as colorants, such as the "vaseline glass" produced in Germany and Bohemia in the 1800s (Miller et

al. 2000 [156684], pp. 75–76). In all cases, the differences in chemistry between borosilicate glass and natural and archeological glasses need to be considered when interpreting analogue data. The qualitative evidence from analogues on natural and archeological glasses has added to confidence that the glass degradation processes are well understood and has provided upper bounding limits to the degradation rates.

4.8 SUMMARY AND CONCLUSIONS

The analogue sites located in chemically oxidizing environments are better analogues to conditions expected to occur at Yucca Mountain than the more numerous sites located in reducing environments. However, some examples from reducing environments may be appropriate analogues for processes that would occur under repository conditions in either type of chemical environment. Hence, both types of conditions were considered in studying the processes relevant to waste form degradation. From the evidence presented in this section, the main points are the following:

- The uranium alteration paragenesis sequence at Peña Blanca is a good analogue to alteration of uranium oxide spent fuel. The reaction path of alteration of spent fuel at Yucca Mountain will be similar to that of geologically young, Pb-free uraninite, with schoepite and becquerelite forming as intermediate products followed by uranyl silicates.
- Measurement of the concentration of fission products as tracers in rock and groundwater surrounding uraninite provides a satisfactory approach to estimating natural dissolution rates. This approach was tested at Cigar Lake and Koongarra under reducing and oxidizing conditions, respectively, and the dissolution rate at Koongarra was found to be more rapid. Use of the fission-product tracer method has not been reported for Oklo, but other lines of evidence indicate that dissolution has been slight under reducing conditions at Oklo over the past approximately 2 billion years. Whether deep oxidizing waters at Okélobondo have increased the dissolution of uraninite as well as created an oxidized suite of minerals is something that could be tested.
- Secondary mineral formation was responsible for incorporating uranium at Shinkolobwe, where 50 secondary uranium-bearing phases could be identified. Because of the great age of the Shinkolobwe uranium deposit, radiogenic lead-bearing phases played a role in sequestering uranium. Lead would not play a role in secondary mineralization of younger deposits, nor would it be present in spent fuel at Yucca Mountain. Other secondary phases, particularly (U,Zr) silicates, formed stable phases at Okélobondo. Presumably radiogenic lead was also present at Okélobondo, because of its approximately 2-billion-year age.
- It is uncertain whether radiolysis will be a potential problem around waste packages in the current design scenario (in which waste packages are not self-shielded). Under radiolysis conditions occurring at the time of reactor criticality at Oklo, only several percent of uranium was estimated to have been mobilized for transport from its original site, under far more extreme conditions than those anticipated at Yucca Mountain. Likewise at Okélobondo, radiolysis effects at the time of reactor operation appear to have been confined to rare earth element migration from mineral core to rim. Because liquid water in

contact with spent fuel is required for radiolysis to occur, the problem seems unlikely under either higher- or lower-temperature operating modes for a potential repository at Yucca Mountain.

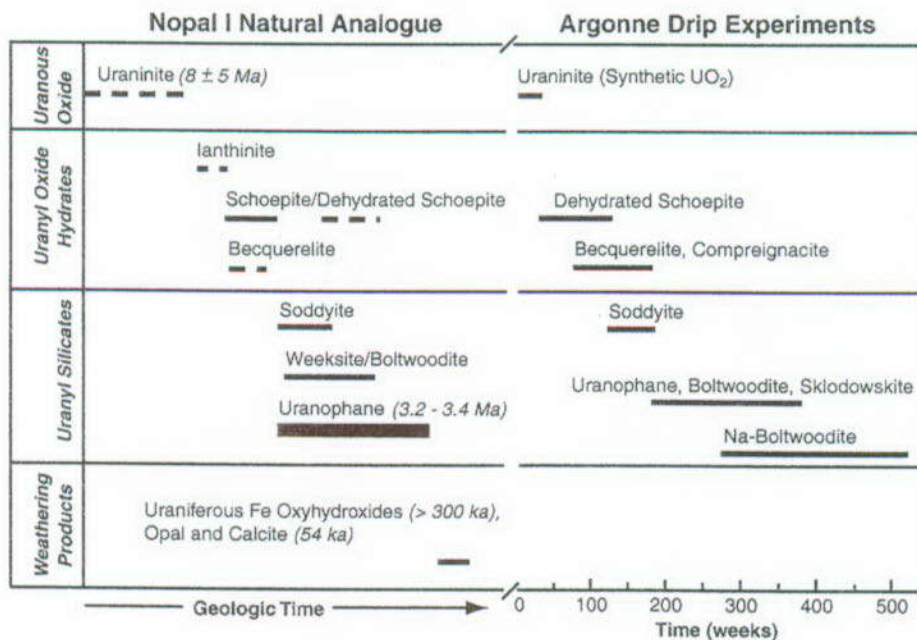
- Criticality of spent fuel can be triggered by changes in pH as well as by reducing conditions. In the study examined, however, criticality was viewed from the standpoint of redox conditions. Criticality of spent fuel, either within waste packages or by reconcentration of uranium outside of the package, has a very low likelihood, because the probability of certain processes required to achieve critical conditions occurring simultaneously or sequentially renders certain conditions mutually exclusive.
- Although natural glasses are somewhat different in composition from borosilicate nuclear waste glass, studies of natural glass alteration indicate that glass waste forms will be stable in a repository environment at Yucca Mountain. Higher stability is favored by higher silica and alumina content and by lower alkali and water content of the glass. Analogue studies have not considered radiation effects on glass over long time periods to confirm experimental results showing that radiation has little effect on glass waste stability.



NOTE: Vegetable matter in lower center is in foreground. Man standing in lower right-center for scale.

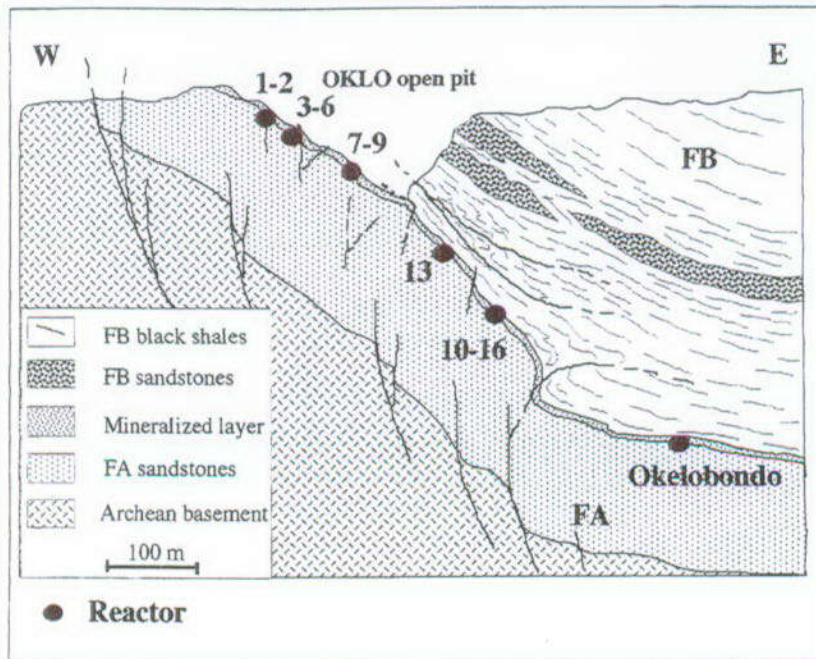
Source: Blanc 1996 [157498], p. III).

Figure 4-1. Photo of a Reactor Zone at the Oklo Natural Fission Reactor, Gabon



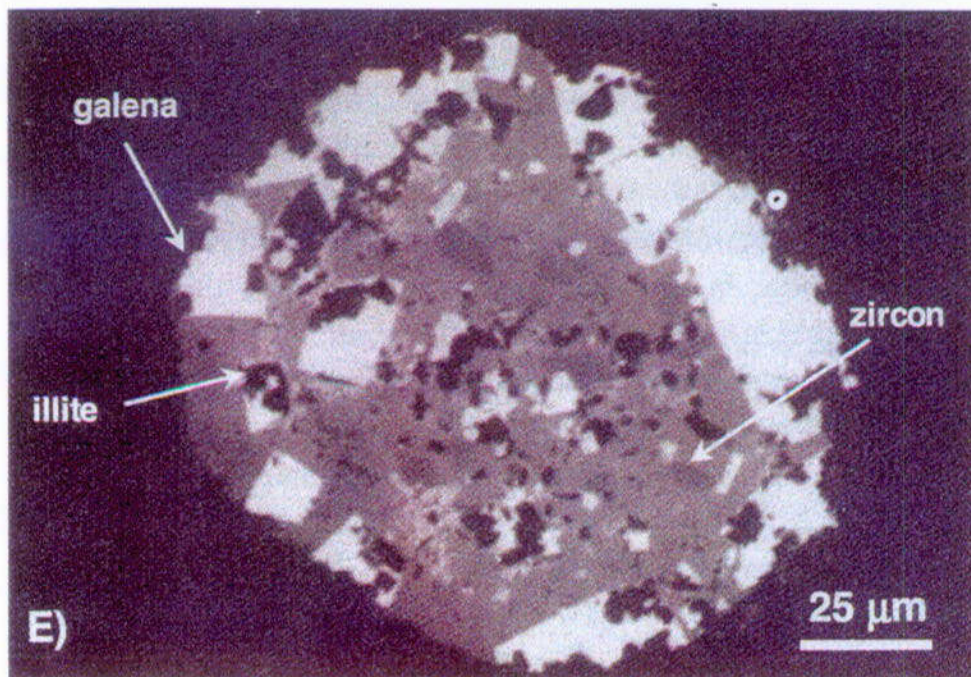
Source: Modified from Murphy 2000 [157487], Figure 1.

Figure 4-2. Sequence of Formation of Uranyl Minerals by Alteration of Uraninite



Source: Gauthier-Lafaye 1996 [157542], Figure 4.

Figure 4-3. Schematic Cross Section Showing Depth of Okélobondo Natural Fission Reactor in Relation to other Oklo Reactors



NOTE: The (U,Zr)-Silicate is the medium gray colored matrix mineral in which the other minerals are encased.

Source: Jensen and Ewing 2001 [157500], Figure 11e.

Figure 4-4. Aggregate of (U,Zr)-Silicate, Zircon, Galena, and Illite in the Center of the Okélobondo Reactor Core (RZOKE)

Table 4-1. Elemental Distribution within Uraninite, Inclusions, and Clays for Elements in the Reactor Zones at Oklo

Element	Uraninite	Inclusions	Clays	Migration
Cs				X
Rb				X
Sr				X
Ba				X
Mo		X		X
Tc		X	X	
Ru		X	X	?
Rh		X	X	?
Pd		X	X	?
Y	X		X	
Nb	?	?		
Zr	X	X	X	
Te		X		
REE	X		X	
Ce		X		
Pb	X	X		X
Bi		X		
Th	X		X	
U	X		X	
Np	?	X		
Pu	X		X	

NOTE: REE-rare earth elements

Source: Miller et al. 2000 [156684], Table 4.2 (summarized from Blanc 1996 [157498]).

5. CURRENT ENGINEERED BARRIER SYSTEM DESIGN

5.1 INTRODUCTION

Section 5 provides a context for Engineered Barrier System (EBS) analogues that are discussed in Sections 6 and 7. This section summarizes the key components of the EBS system and describes the materials proposed to be used in the construction of these components. Finally, the key processes that are expected to occur during the operational life span of the EBS are described.

5.2 EBS COMPONENTS

The EBS currently planned for the potential Yucca Mountain repository (Figure 5-1) consists of three main components: (1) drip shield, (2) emplacement drift invert, and (3) waste package (DOE 2001 [153849], Section 2.4). Because they will affect the performance of the EBS, materials included within the waste forms and used in the construction of the emplacement drifts also are considered in the evaluation of the EBS. The following summary of the components of the EBS system is based upon Sections 2.4 and 3 of the *Yucca Mountain Science and Engineering Report (S&ER)* (DOE 2001 [153849]).

5.2.1 Drip Shield

The drip shield is designed to serve as a protective barrier, for the length of emplacement drifts, that will divert water dripping from the drift walls, thus minimizing direct dripping onto the waste packages. The drip shield has the added function of protecting the waste package from rock falls from the drift perimeter. These functions require that the drip shield assembly is both highly resistant to corrosion and has the structural strength to withstand rock falls.

The drip shield consists of three separate elements: the drip shield, supporting structural members, and stands (or "feet") upon which the shield assembly rests (Figure 5-2). Current design plans call for the drip shield to be manufactured from 15 mm (0.6 in.) thick Titanium Grade 7 plates for long-term corrosion resistance. The structural members will be constructed using Titanium Grade 24, which has greater strength than Titanium Grade 7. Alloy 22 (see Table 5.2) will be used for the feet, preventing direct contact between the titanium structural members and the carbon steel beams of the invert.

5.2.2 Drift Invert

The drift invert is designed to form a stable, level platform along the base of the emplacement drift on which the waste package and drip-shield assemblies will be placed. The invert as currently planned (DOE 2001 [153849], Section 2.4.1) consists of two components: a steel invert structure and a crushed-tuff invert ballast.

The steel invert structure needs to provide sufficient support for all expected pre-closure activities for up to 300 years and must also keep the waste packages in a horizontal position for 10,000 years after closure. The steel structure consists of transverse and longitudinal support beams, which serve to transfer the weight of the waste package and drip shield (along with any

needed emplacement and maintenance equipment during the initial phases of operation) to the bedrock (Figure 5-3). Gantry rails, needed to transport the waste packages and drip shields into the tunnel, will be placed along the margins of the support beam structure. Guide beams will be used (if considered necessary to mitigate movement resulting from seismic events) to secure the waste package emplacement pallets and the drip shield assembly. The current design calls for the invert support and guide beams to be manufactured of ASTM A 572/A 572M steel, which was chosen to provide sufficient strength for the emplacement drift environment. The gantry rail will be made of ASTM A 759 carbon steel (DOE 2001 [153849], Section 2.4.1.1).

The invert ballast is designed so that moisture present in the emplacement drift will drain directly into the surrounding rock without flowing along the base of the drift. Crushed tuff, produced by crushing material obtained during the excavation of the emplacement drifts, would be used as the primary ballast material. The ballast will be placed around the steel invert beams, to a level just below the top of the support beams, so that the waste package pallets and drip shields rest on the support beams and not on the ballast. The ballast material will be compacted so that no significant settling will occur over time. The crushed tuff should not be affected by heating related to emplacement of the waste packages. Transport of radionuclides within the crushed tuff is expected to be dominated by diffusive transport, thus serving to retard any potential release of radionuclides into the surrounding host rocks (DOE 2001 [153849], Section 2.4.1.2).

5.2.3 Waste Package

The waste package assembly is designed to securely contain high-level radioactive wastes and serve as the primary element to the EBS. The waste package system consists of two main components: a waste package emplacement pallet and a sealed, corrosion-resistant waste package canister (Figure 5-4).

The waste package emplacement pallets are designed to support the waste package canisters in a horizontal position and facilitate line-loading of the waste packages. Current plans call for the pallets to be manufactured from plates of Alloy 22 (a material highly resistant to corrosion) with support tubes fabricated from Stainless Steel Type 316L (DOE 2001 [153849], Section 2.4.3.1). The V-shaped design will allow the pallets to be used for all waste package canisters.

A number of distinct waste package designs have been developed to accommodate the different waste forms generated from boiling water and pressurized water reactors, excess weapons material, high-level waste, and DOE and naval spent nuclear fuel (Figure 5-5). All of these waste package designs contain a number of important components that are needed to meet performance criteria. The performance criteria (DOE 2001 [153849], Section 3.4.1) are as follows:

- Strength
- Resistance to corrosion and microbial attack
- Predictable materials behavior
- Compatibility with waste package and waste form materials
- Ease of fabrication
- Proven performance record
- Favorable heat transfer properties
- Utility in shielding and preventing criticality.

Table 5-1 lists the major waste package components for commercial spent nuclear fuel waste packages, the composition of each component, and the component function(s).

The different materials chosen for the construction of the waste package system are based on the functional requirements for each component. Key properties include resistance to corrosion and cracking caused by thermal, mechanical, and chemical processes; preservation of the structural integrity of the waste package system; conduction of heat away from the waste forms; and the ability to prevent criticality from occurring. A brief description of each of the main types of materials incorporated in the current design (DOE 2001 [153849], Section 3) is given below.

5.2.3.1 Corrosion-Resistant and Structural Materials

Alloy 22 was selected for the outer barrier of the waste package because of its resistance to corrosion under conditions of high temperatures and low humidity and under all low-temperature conditions, its similar thermal expansion coefficient to stainless steel, and because it can be welded more easily than can titanium. The chemical composition of Alloy 22 is given in Table 5-2. Stainless Steel Type 316NG was chosen for the inner cylinder of the waste package because of its relative strength, compatibility with Alloy 22, and its affordability. The chemical composition of Stainless Steel Type 316NG is given in Table 5-3.

5.2.3.2 Other Waste Package Materials

A variety of other materials will be used in the fabrication of the waste package assembly (DOE 2001 [153849], Section 3.2.2.1). These include Neutronit A 978 (borated 316 stainless steel) or SA 516 Grade 70 carbon steel plates, boron carbide rods with Zircaloy cladding used for control of criticality within the waste package container, and aluminum shunts (SB-209 6061 T4) to assist in heat transport away from the waste form. The waste package will encompass the waste form materials described in Section 5.2.4.

5.2.4 Waste Form Components

The waste forms for disposal at the potential Yucca Mountain repository include spent fuel from commercial power reactors and that owned by the U.S. Department of Energy, solidified high-level radioactive waste, and plutonium waste from excess nuclear weapons. All waste must be in solid form and must not contain flammable or chemically reactive materials. The waste forms will contain fuel rods constructed out of Zircaloy and stainless steel as well as a variety of radioactive waste types, including uranium metal, uranium oxide, uranium dioxide, radioactive borosilicate glass, and plutonium encased in ceramic pellets (DOE 2001 [153849], Section 3). Analogues to waste form materials and their degradation are discussed in Section 4.

5.2.5 Emplacement Drifts

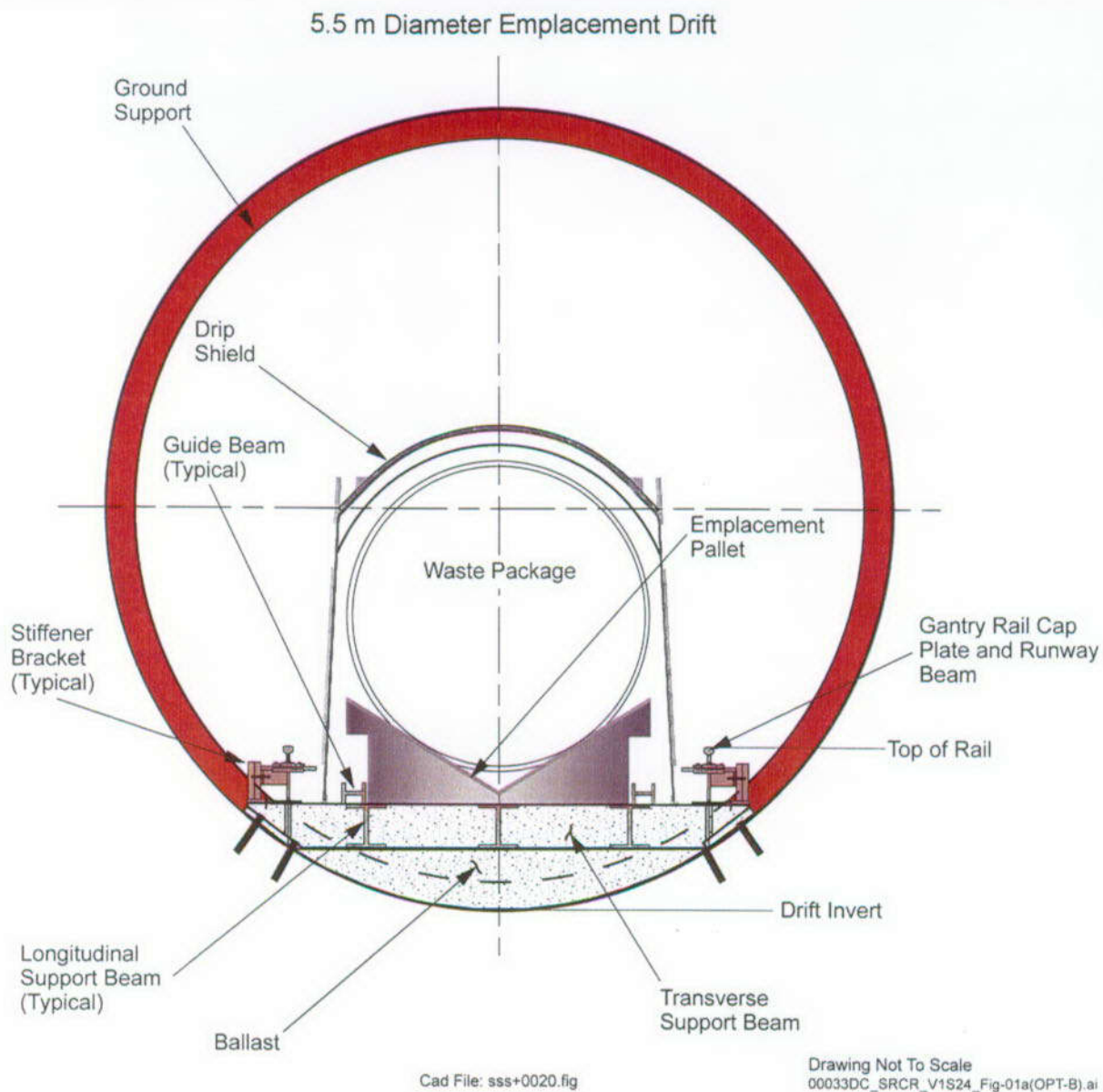
While the emplacement drifts are not considered a component of the engineered barrier system, the materials used in their construction could significantly affect the EBS performance. The emplacement drifts contain a variety of materials that are used to help maintain the integrity of the drift after excavation. The ground support system, designed to stabilize the emplacement drift, includes W6X20 rolled steel ring beams (steel sets), tie rods, welded wire fabric, rock bolts,

and cementitious grout used to secure the rock bolts in place (DOE 2001 [153849], Section 2.3.4.1.2.1). Analogues relevant to emplacement drift components are discussed in Section 7.

5.3 PROCESSES AFFECTING EBS PERFORMANCE

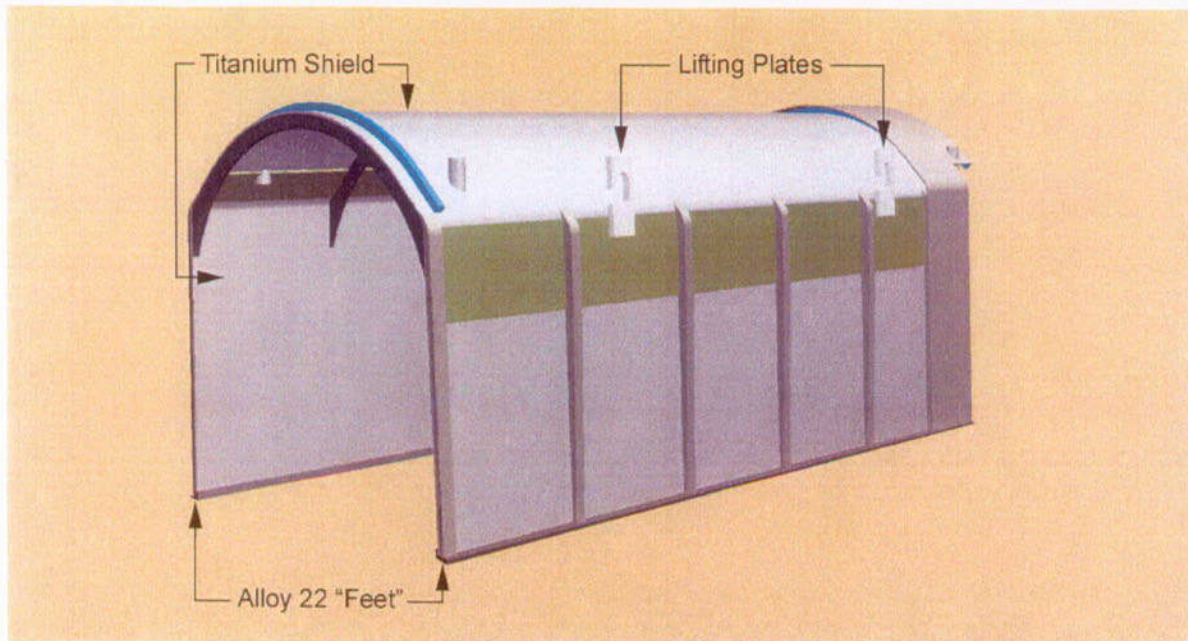
Numerous processes and event scenarios have been identified and considered in designing the EBS (DOE 2001 [153849], Sections 2.4 and 3.1). These can be grouped into four major categories: structural, thermal, chemical, and nuclear criticality. The structural events evaluated involve scenarios (such as mishandling of the packages, seismic events, or rock falls) that would result in the waste package being physically disturbed by an impact that could potentially result in breaching the sealed waste packages. Thermal processes include changes in physical and chemical properties associated with heating caused by radioactive decay of the waste forms, such as thermal expansion and cracking, as well as the effects of heat transfer properties. Chemical processes such as corrosion and chemical reaction of the different materials could also result in breaching of the sealed waste packages and subsequent release of radionuclides into the surrounding environment. Special attention has been placed on the design of the waste packages and composition of the waste forms to prevent the radioactive waste from achieving criticality. The selection of the different materials used in construction of the EBS components has been made to ensure the long-term structural, thermal, and chemical integrity of the waste packages and to prevent the waste forms from going critical.

While the properties of all of the materials selected for the EBS design have been extensively tested and determined in the laboratory, the long-term performance of these materials under the predicted temperature, humidity and chemical environment for the potential Yucca Mountain repository has not been experimentally confirmed. Natural analogues for similar materials found in the natural environment can be used to validate long-term performance models for the EBS. The following sections (6 and 7) provide descriptions of natural analogues for waste package materials and for processes that might take place within the EBS.



Source: DOE 2001 ([153849], Figure 2-71).

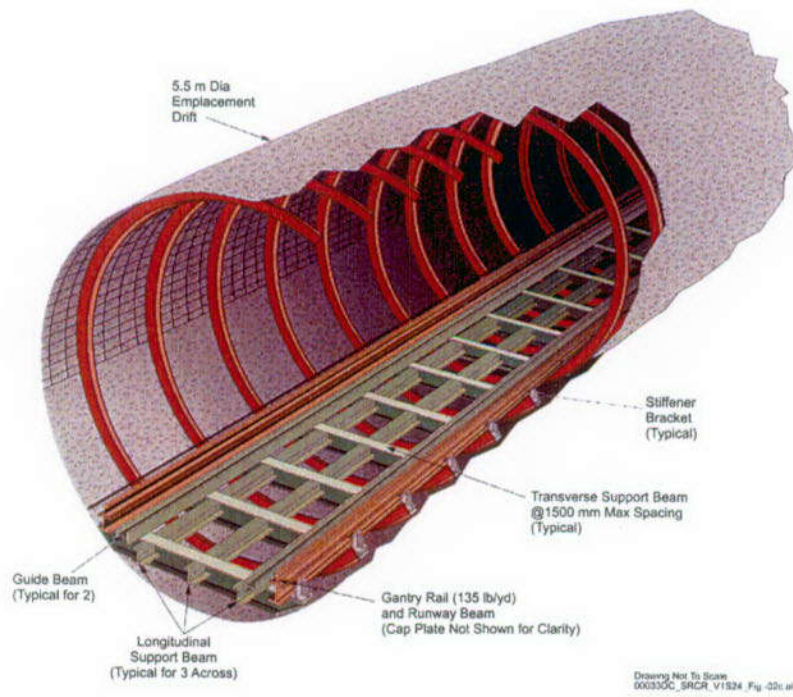
Figure 5-1. Cross Section of Emplacement Drift with EBS Components



Drawing Not To Scale
00033DC_ATP_Z1S24_Fig-03a cdr

Source: DOE 2001 ([153849], Figure 2-73).

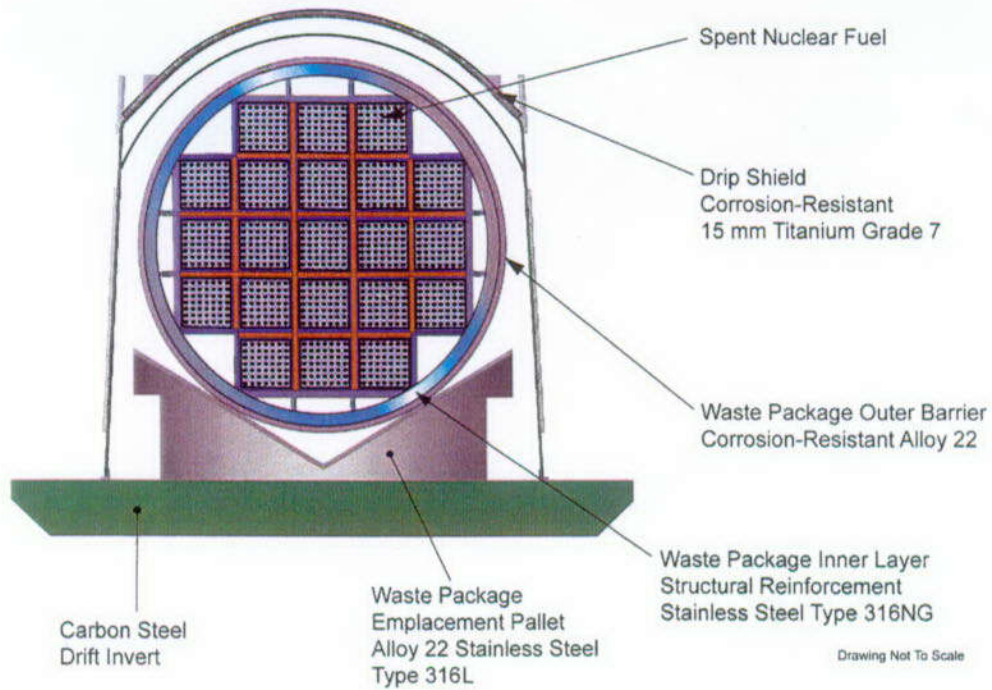
Figure 5-2. Schematic View of Drip Shield Assembly with Drip Shield, Support Members, and Feet



Drawing Not To Scale
00033DC_SRCR_V1S24_Fig-02i.ai

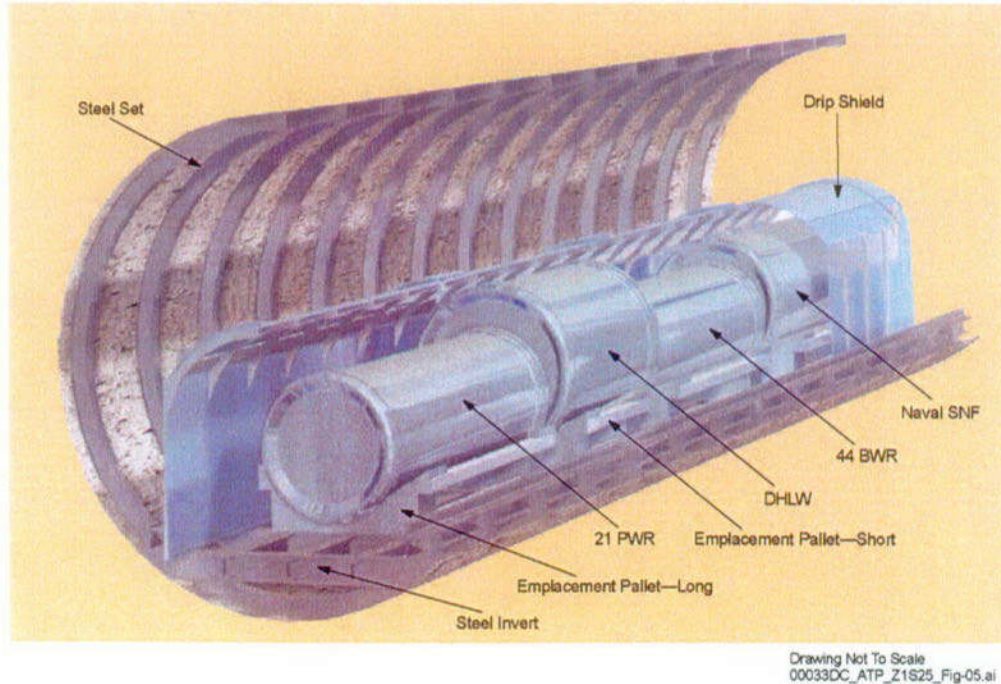
Source: DOE 2001 ([153849], Figure 2-72).

Figure 5-3. Perspective View of Steel Invert Structure in Emplacement Drift



Source: DOE 2001 ([153849], modified from Figure 3-1).

Figure 5-4. Cross Section of Waste Package, Emplacement Pallet, and Drip Shield



NOTE: PWR = Pressurized Water Reactor; DHLW = Defense High-Level Radioactive Waste; BWR = Boiling Water Reactor; and SNF = Spent Nuclear Fuel. Source: DOE 2001 ([153849], Figure 2-77).

Figure 5-5. Schematic View of Different Waste Packages in Emplacement Drift

Table 5-1. Commercial Spent Nuclear Fuel Waste Package

Component	Composition	Function
Outer barrier and lids	Alloy 22	Protect against corrosion
Support ring	Alloy 22	Hold inner cylinder in place
Inner structural shell and lid	Stainless Steel Type 316NG	Provide structural integrity
Waste package fill gas	Helium	Heat conductor, with need to be compatible with spent fuel
Fuel tubes for internal basket	Carbon steel (SA 516 Grade 70)	Hold fuel assemblies in place and provide structural strength and conduct heat away from cladding
Interlocking plates for internal basket	Carbon steel (SA 516 Grade 70)	Provide structural strength to maintain fuel geometry and prevent criticality
Neutron absorber materials for internal basket	Neutronic A 978 (borated 316 stainless steel)	Prevent criticality, provides structural strength and conduct heat away from waste form to walls of waste package
Thermal shunts for internal basket	Aluminum alloy (SB-209 6061 T4)	Transfer heat from waste form to walls of waste package
Structural guides for internal basket	Carbon steel (SA 516 Grade 70)	Provide structural strength to hold basket structure in place and prevent criticality, conduct heat to walls of waste package
Control rods	Boron carbide with Zircaloy cladding	Provide long-term criticality control

Source: DOE 2001 [153849], modified from Table 3-9, Sections 3.1 and 3.2.2.

Table 5-2. Chemical Composition of Alloy 22

Element	Composition (wt %)
Nickel	50 to 63
Chromium	20.0 to 22.5
Molybdenum	12.5 to 14.5
Iron	2.0 to 6.0
Tungsten	2.5 to 3.5
Cobalt	2.50 (max)
Manganese	0.50 (max)
Vanadium	0.35 (max)
Silicon	0.08 (max)
Phosphorus	0.02 (max)
Sulfur	0.02 (max)
Carbon	0.015 (max)

Source: DOE 2001 [153849], modified from Table 3-12.

Table 5-3. Chemical Composition of Stainless Steel Type 316NG

Element	Composition (wt %)
Iron	61 to 71
Chromium	16.00 to 18.00
Nickel	11.00 to 14.00
Molybdenum	2.00 to 3.00
Manganese	2.00 (max)
Silicon	0.75 (max)
Copper	0.50 (max)
Cobalt	0.10 (max)
Vanadium	0.1 (max)
Nitrogen	0.06 to 0.10
Titanium	0.05 (max)
Tantalum and Niobium	0.05 (max)
Aluminum	0.04 (max)
Phosphorus	0.030 (max)
Carbon	0.020 (max)
Bismuth + Tin + Arsenic + Lead + Antimony + Selenium	0.02 (max)
Sulfur	0.005 (max)
Boron	0.002 (max)

Source: DOE 2001 [153849], modified from Table 3-13.

6. WASTE PACKAGE DEGRADATION ANALOGUES

6.1 INTRODUCTION

This section describes the use of natural analogues to evaluate the long-term performance of metals used in the fabrication of waste packages for storage of high-level radioactive waste. Key concerns for the waste package materials (described in Section 5) include the possible degradation and corrosion of metals caused by mechanical stress, hostile physical and chemical environments, and metallurgical factors. The primary degradation and corrosion issues expected for Yucca Mountain include elevated temperature and humidity, and contact with seepage water that could have corrosive chemistry. A number of different analogues were previously discussed in Chapter 13 of the *Yucca Mountain Site Description* (CRWMS M&O 2000 [151945], Section 13.3.5); those analogues applicable to the waste materials described in Section 5 are briefly summarized below. Additional analogue examples are discussed in more detail in the following subsections.

The long-term stability of the waste package materials is directly related to repository environmental conditions. Preservation of delicate archaeological materials, including metals, appears to be enhanced by their location in an arid or semi-arid unsaturated environment (CRWMS M&O 2000 [151945], Section 13.3.4). Mummified remains 4,000 to 8,000 years in age were recently discovered in shallow burial pits in the high Andes Mountains of Chile. The Dead Sea scrolls were preserved in caves along the shores of the Dead Sea for over 2,000 years. All of these artifacts have survived millennia, and their preservation is attributed in part to being in arid to semiarid unsaturated environments (Winograd 1986 [127015], p. 8).

Metal analogues, involving both naturally occurring and archaeological objects, were also described in the *Yucca Mountain Site Description* (CRWMS M&O 2000 [151945], Section 13.3.5). A cache of Roman iron nails was recovered after almost 1,900 years of burial in Scotland (Miller et al. 1994 [126089], pp. 114–119). Corrosion of the outermost nails formed a protective rust rind, serving to create a more reducing (and thus more stable) environment for the innermost nails. Using a variety of iron archaeological artifacts, Johnson and Francis (1980 [125291], Fig. 3-1) calculated general corrosion rates of 0.1 to 10 $\mu\text{m}/\text{yr}$ for most of the artifacts under a range of environmental conditions. Iron meteorites often have poorly constrained exposure histories, but differential corrosion of different mineral phases can be used to estimate relative resistance to corrosion, suggesting that Ni-rich phases (taenite and schreibersite) are more stable than Fe-rich phases (Johnson and Francis 1980 [125291], p. 4.23). Copper-bearing archaeological artifacts, such as sunken and buried bronze cannons, can also be used to estimate general corrosion rates over extended (hundreds to thousands of years) periods of time. These metal analogues, while differing in chemical composition from the waste package films, provide important insights into the way different metals survive corrosion over long time periods, and illustrate the importance of passive films.

Most of the metals being considered for use in the waste packages at a potential Yucca Mountain repository consist of alloys that do not occur naturally and are not present in the archaeological record (see Tables 5-1 to 5-3). However, the long-term behavior of metals with similar compositions that are present either as minerals or as man-made objects can be used to build

confidence in long-term performance models of the waste package materials. Analogues to long-term behavior of metals related to waste package materials are described in Section 6.2.3. Information found in Section 6.2 may help to support arguments associated with Key Technical Issue (KTI) KUZ0407 listed in Table 1-1.

6.2 NATURAL ANALOGUE STUDIES OF CORROSION

This section will discuss new work on some of the natural analogues previously summarized in Chapter 13 of the *Yucca Mountain Site Description* (CRWMS M&O 2000 [151945]), as well as present information on examples not previously discussed in the Site Description.

6.2.1 Environmental Factors Related to Corrosion

Knowledge of the in-drift physical and chemical environment at Yucca Mountain is critical in predicting the long-term performance of waste packages and the EBS. Processes such as the evaporation and condensation of water, precipitation and dissolution of salts, seepage and mass transport of materials into the drift environment, and the abundance, compositions, and reactions between solid, liquid, and gas phases will affect the physical and chemical integrity of waste packages and other EBS components.

One of the key attributes of the potential Yucca Mountain repository is its location within the unsaturated zone, thus reducing the amount of water that can come into contact with waste packages. Previous reviews of natural analogues of caves within the unsaturated zone have demonstrated that very old archaeological artifacts can be preserved in such environments (CRWMS M&O 2000 [151945], Section 13.3.4). Hundreds of wooden and reed fragments of dart and arrow shafts (dated between 3,300 to 9,300 years B.P.) have been recovered from Pintwater Cave in southern Nevada (Buck and DuBarton 1994 [157438], pp. 228, 239). These delicate items were collected from the limestone cave floor and in a test pit excavated within eolian sediments lining the floor of Pintwater Cave (Buck and DuBarton 1994 [157438], p. 226), and their preservation suggests that they were not subjected to prolonged exposure to water. However, as shown in the following example, the maintenance of a stable microclimate is a critical feature in making caves suitable for long-term preservation.

The Altamira cave, located in northern Spain, is the site of Paleolithic cave paintings (Sanchez-Moral et al. 1999 [157382]). Since the discovery of the prehistoric cave art in 1879, significant degradation of the cave paintings has occurred, leading to the cave being closed to the public in 1977. The cave was reopened in 1982 with fixed limits on the number of visitors. Continuous monitoring of the Altamira cave microclimate within Polychromes Hall (a cave chamber with famous polychromatic paintings) during 1997–1998 determined that increases in temperature ($\Delta = +0.25^\circ\text{C}$) and CO_2 concentrations ($\Delta = +500$ ppmv) resulted directly from the presence of visitors in the cave (Sanchez-Moral et al. 1999 [157382], p. 78).

Sanchez-Moral et al. (1999 [157382]) used these data to estimate effective calcite corrosion rates for both the baseline and modified (visitor-related case) cave conditions. They predicted that the visitor-induced temperature increase (resulting from radiation of body heat) will greatly increase the amount of water condensation occurring on the cave walls and ceiling. The elevated P_{CO_2} (partial pressure of carbon dioxide) conditions caused by human respiration, combined with the

higher amounts of condensation, were predicted to result in visitor-induced corrosion rates (314 mm³/yr) in Polychromes Hall that are 78 times higher than the baseline (no visitor) case

(Sanchez-Moral et al. 1999 [157382], p. 78). As noted by visual observation and modeling, the relatively minor changes in temperature and P_{CO_2} at Altamira had a significant impact on deterioration of the cave art. Thus, the corrosion-resistance properties of waste package materials at Yucca Mountain need to be evaluated for all possible variations in environmental conditions during the postclosure period.

One critical factor affecting the chemical integrity of the waste packages is the potential development of hypersaline fluids within emplacement drifts at Yucca Mountain. Such fluids could be generated by evaporative concentration of dissolved salts in pore waters in the near-drift environment caused by heating, or by dissolution of previously formed salts in the dryout zone around the drift by downward percolating condensate waters and/or surface infiltration. The amount and salinity of water in contact with waste packages depend on a number of factors, including evaporation, condensation, temperature, and fluid flux rates into the emplacement drifts (Figure 6-1). Conceptual and numerical models of these processes suggest that fluid compositions within the emplacement drifts may be highly variable over time (Walton 1994 [127454], pp. 3483–3486).

To constrain models involving the generation of hypersaline fluids at Yucca Mountain, Rosenberg et al. (2001 [154862]) conducted a series of experiments at sub-boiling temperatures (75–85°C) to evaluate the evaporative chemical evolution of pore water from the unsaturated zone and of well water from the saturated zone at Yucca Mountain. Synthetic solutions of these two fluid types were evaporated, with samples collected and analyzed after approximately 100 and 1,000 × evaporative concentration and evaporation to dryness (Table 6-1). A number of different minerals formed from complete evaporation of these waters, including amorphous silica, aragonite, calcite, halite, niter, smectite, thermonatrite, tachyhydrite, and gypsum. The groundwater (obtained from the J-13 well at Yucca Mountain) composition evolved into a high pH, sodium carbonate-bicarbonate brine resulting from the precipitation of calcium-magnesium carbonate, while the UZ pore-water composition evolved into a near-neutral pH, sodium-potassium-calcium-magnesium-chloride-nitrate brine resulting from the precipitation of gypsum. Different fluid chemistry may develop under higher temperature (boiling) conditions as a result of CO_2 degassing, which could have an important impact on the pH of the evolved fluids. These experimental results provide a data set against which to compare brines from analogue sites that have interacted with metals in a natural environment.

Hypersaline fluids, such as those encountered at the Salton Sea geothermal field (Table 6-2), have been observed to aggressively corrode many steel compositions (McCright et al. 1980 [157384], pp. 646–648). Carbon steel drill casings initially used in geothermal production wells at the Salton Sea field experienced general corrosion rates as high as 25.4 mm/yr, with even higher localized corrosion rates observed (Pye et al. 1989 [157385], p. 260). These rates are much higher than the rates of 10–40 $\mu\text{m}/\text{yr}$ obtained by Ahn and Soo (1995 [104751], p. 475) for corrosion tests of A216-Grade WCA low-carbon steel in concentrated synthetic groundwater solutions. The differences in corrosion rates likely result from: (1) differences in steel compositions; (2) higher temperatures for the Salton Sea fluids (232–315°C) than those used for the corrosion experiments (80–150°C); and (3) much higher salinities for the Salton Sea brines (150,000–300,000 ppm TDS) relative to the synthetic experimental brines (7,455 ppm TDS). Corrosion problems at the Salton Sea were successfully mitigated through the use of a corrosion-resistant titanium alloy (see Section 7.2.1). The current drip shield design for Yucca

Mountain (see Section 5.2.1) calls for the use of titanium because of its corrosion-resistant properties.

Another concern for waste package materials is the possible evaporative concentration of minor dissolved constituents, such as arsenic, lead, and mercury, that could enhance corrosion (BSC 2001 [155950], Section 7.3.1.3.4; [157151], Appendix E, Section 3.1.2). The hypersaline Salton Sea brines have significant concentrations of arsenic (8 ppm) and lead (66 ppm). However, groundwaters in the vicinity of Yucca Mountain have only trace amounts of lead, with a median concentration of 9 ppb (Lee 2001 [155241]; Perfect et al. 1995 [101053]). Two samples of J-13 well water from Yucca Mountain were analyzed for lead, with one sample yielding a value of 3 ppb, while the other was below detection (BSC 2001 [155950], Section 7.3.1.3.4; Perfect et al. 1995 [101053]). Lead concentrations in groundwater at Yucca Mountain may be limited by precipitation of lead in the form of carbonate, oxide, or sulfide minerals, or by sorption onto mineral surfaces (BSC 2001 [155950], Section 7.3.1.3.4, [157151], Appendix E, Section 3.1.2). Evaporative concentration of water in the near-drift environment at Yucca Mountain could result in higher lead concentrations. However, even a 1,000-fold increase in lead concentration in J-13 water would still only result in a brine with ~3 ppm lead, over 20 times lower than the concentrations observed in Salton Sea brines. Thus, the very low concentrations of lead in groundwater at Yucca Mountain greatly reduce the risk that lead (and other trace metals) could pose to the chemical integrity of the waste packages.

6.2.2 Passive Film Formation

The formation of passive films has a significant impact on the corrosion-resistant properties of metals and metal alloys (BSC 2001 [155950], Section 7.3.4). Passive films are stratified coatings consisting of an inner oxide layer and an outer layer of hydroxide or oxyhydroxide (Macdonald 1992 [154720], pp. 3434–3437; Marcus and Maurice 2000 [154738], pp. 145–152). The inner layer forms a corrosion barrier, while exchange occurs within the outer layer of the passive film. These films act as semiconductors or insulators, thus reducing the rate of metal dissolution triggered by an electrochemical potential between a metal and its surrounding electrolyte solution.

The Delhi iron pillar is a 1,600-year old metal artifact (Figure 6-2) that has withstood exposure to the atmosphere with only relatively small amounts of corrosion. Study of the rust layer coating the pillar reveals the presence of crystalline iron hydrogen phosphate hydrate and amorphous iron oxyhydroxides and magnetite (Balasubramaniam 2000 [157383], pp. 2115–2116). The low-porosity crystalline phosphate phase forms a passive film around the pillar, serving to protect it from further corrosion (Figure 6-3). Balasubraminiam (2000 [157383], pp. 2112–2115) interpreted the presence of ~0.25 wt% phosphorous and fine slag particles in the iron to be critical to the development of the corrosion-resistant layer.

6.2.3 Naturally Occurring Metals as Natural Analogues

Josephinite—Josephinite, a naturally occurring Ni-Fe-Co metal-bearing rock consisting of the minerals Ni_3Fe (awaruite), andradite garnet, FeCo (wairuite), and minor to trace amounts of Ni_6Fe_4 and $\text{CaO}\cdot 2\text{FeO}$ (calciowüstite), is a possible natural analogue for Ni-Fe alloys (similar to Alloy 22, which is a Ni-Cr-Mo-W alloy) proposed for the Yucca Mountain waste packages. The

type locality of josephinite is the Josephine Ophiolite, a ~150 million-year-old serpentinized ultramafic body in Oregon, where it occurs within serpentine veins and as coarse metallic nuggets in nearby placer deposits (Dick 1974 [154749]). Josephinite was interpreted by Dick (1974 [154749], p. 297) to be a product of hydrothermal alteration and serpentinization of peridotite. Josephinite and awaruite are very stable rock and mineral phases, as evidenced by their survival for millions of years with only minor amounts of oxidation. Because of this long-lived stability, these ordered Ni-Fe-Co metals (Bassett et al. 1980 [157531]) have been proposed as alloys in constructing containers for the storage of high-level radioactive waste (Bird and Ringwood 1980 [157397]; 1982 [157398]; 1984 [157396]).

Relatively unaltered masses of metal that are predominantly Ni_3Fe (with small inclusions of Ni_3As) were discovered in 1999 within harzburgite in the Josephine Ophiolite and as eroded blocks up to ~3 kg (Bird 2001 [157514]). Preliminary Pb and Os isotopic analyses of these new samples suggest that the josephinite metal did not form as an alteration product of the Josephine Ophiolite, but instead may represent xenoliths within the serpentinite body that have a deep-mantle origin (Bird 2001 [157514]).

The josephinite nuggets have alteration rims comprised of Fe_3O_4 (magnetite, with maghemite) and NiFe_2O_4 (trevorite). Some samples of josephinite contain the high-temperature phase taenite (a disordered Ni-Fe metal) in addition to awaruite (BSC 2001 [155950], Section 7.3.2.4.2). Phase relation studies of the Fe-Ni system suggest that taenite is not stable below ~350°C, and that α -Fe, pure Ni, and awaruite are the stable phases for this system at ambient temperatures (Botto and Morrison 1976 [154716], p. 264). The persistence of taenite for millions of years suggests that low-temperature phase change rates for taenite are exceedingly slow (BSC 2001 [155950], Section 7.3.2.4.2). X-ray photoelectron spectroscopic analysis of a josephinite placer sample from the Josephine Ophiolite (Figure 6-4) revealed that while both iron and nickel are oxidized on the surface, nickel remains in reduced (metallic) form at depths of 2 nm and greater (analyzed to a depth of 120 nm), indicating that the bulk sample has not undergone significant amounts of oxidation (BSC 2001 [157151], Appendix E, Section 3.3.2, Table 1). Because of its high nickel concentrations, the longevity of josephinite indicates that nickel alloys will have long-term phase stability. While josephinite does not contain the molybdenum and tungsten that serve as stabilizing elements in Alloy 22 passive films, its ability to resist corrosion provides confidence that Alloy 22 will remain passive under potential repository conditions (BSC 2001 [157151], Section 3.3.2, Appendix E).

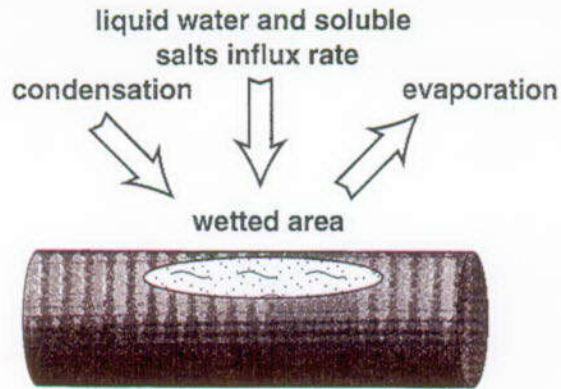
Chromite—Analogues for chromium are considered because of the chromium content of Alloy 22 (Table 5.2). Chromium occurs in minerals in the form of chromite (FeCr_2O_4) and chromium spinel ($\text{Mg}(\text{Cr},\text{Al})_2\text{O}_4$). These Cr-bearing minerals are typically found in mafic and ultramafic rocks. Elevated concentrations of chromium in groundwaters in the Leon-Guanajuato valley of central Mexico have been attributed to weathering and alteration of chromite from ultramafic rocks of the Sierra de Guanajuato that have been interpreted to be Jurassic in age (Robles-Camacho and Armienta 2000 [157386], pp. 172–173, 178–181). The San Juan de Otates pyroxenite unit consists of pyroxenite and serpentinized peridotite, harzburgite, and wehrlite. Discrete concentrations of ilmenite and chromite occur within these rocks, and form subrounded masses in outcrop. Chromite is typically found as subrounded crystals, often with exsolution borders of magnetite.

A variety of ultramafic rock samples from the Sierra de Guanajuato, with total chromium contents ranging from 55 to 4115 ppm, were leached with acid to evaluate the susceptibility of the rocks to weathering and subsequent release of chromium (Robles-Camacho and Armienta 2000 [157386], pp. 173–181). The laboratory acid treatment was designed to examine (over a much shorter time scale and under much more acidic conditions than found in the field) the effects of weathering resulting from interaction of oxygenated, CO₂-rich groundwater with chromium-bearing minerals (Robles-Camacho and Armienta 2000 [157386], pp. 174–177). The leachate from Cr-rich serpentinite samples yielded the highest concentrations (up to 274 mg Cr/kg rock), suggesting that they have the greatest potential to release chromium. SEM analysis of samples examined after leaching suggests that dissolution occurred along magnetite exsolution borders of chromite grains (Figure 6-5). Total chromium contents of groundwater samples collected from wells, streams, and reservoirs near the ultramafic rocks range up to 0.0149 mg/L. The Ca-Mg-HCO₃ composition of these waters is consistent with interaction with serpentinized ultramafic rocks. The study does not provide information on the rates of chromite weathering, but it does indicate that chromite exsolution borders are susceptible to chemical attack. This observation is analogous to localized corrosion and pitting observed in metals along structural defects.

6.3 SUMMARY

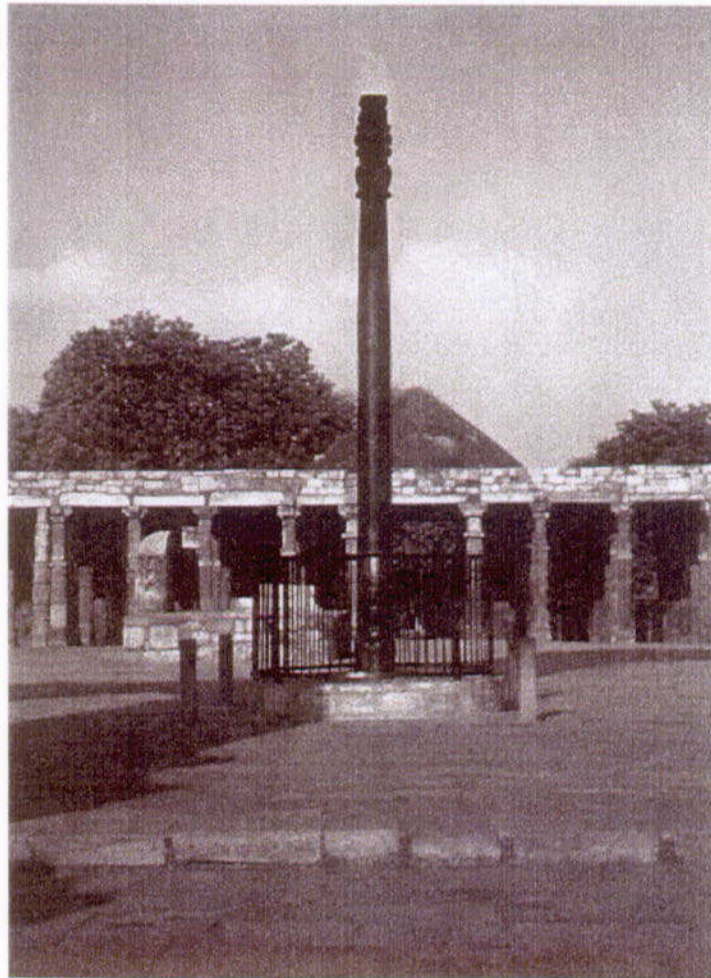
1. The survival of metal archaeological artifacts over prolonged periods of time is related to the corrosion-resistant properties of metals and metal alloys, the development of protective passive film coatings with the onset of corrosion, and the location of artifacts in arid- to semi-arid environments. Such features can be used in the selection of materials and design configuration to enhance the durability of waste packages at Yucca Mountain.
2. Archaeological examples, such as the Altamira cave, illustrate how environmental changes can significantly affect corrosion behavior. A wide variety of environmental conditions is expected to occur in the near-drift environment at Yucca Mountain during the lifespan of the repository. The introduction of heat-generating waste packages and EBS materials into drifts will perturb the existing physical and chemical system at Yucca Mountain. The materials used for the waste packages (and the rest of the EBS) need to withstand the predicted adverse changes in environmental conditions.
3. Small volumes of concentrated brines could develop in the near-drift environment as a result of evaporation and later dissolution of precipitated salts in the dryout zone with rewetting. High-salinity fluids pose a significant corrosion hazard to carbon steel, as seen at the Salton Sea geothermal field, but the use of titanium alloys can effectively minimize this hazard.
4. The survival for millions of years of the naturally occurring ordered Ni-Fe alloy found in josephinite (with only relatively minor amounts of surface oxidation) indicates that this material is highly resistant to oxidation and other forms of corrosion that occur in its geologic environment. While the composition of this metal differs from Alloy 22 (in that it does not contain Cr, Mo, and W), it does provide evidence that a similar alloy can remain passive over prolonged periods of time.

5. The potential instability of chromium-bearing materials is illustrated by the observed natural release (under ambient conditions) of chromium from chromite in the Sierra de Guanajuato ultramafic rocks. Corrosion appears to be concentrated along exsolution rims, analagous to structural defects on metal surfaces. While the chromite has undergone some alteration, it has survived for over 140 m.y. (since Jurassic time). The corrosion behavior of this chromium oxide mineral may differ from that of the chromium-bearing metal alloys (Section 5) that are currently slated for use in the construction of the waste package.



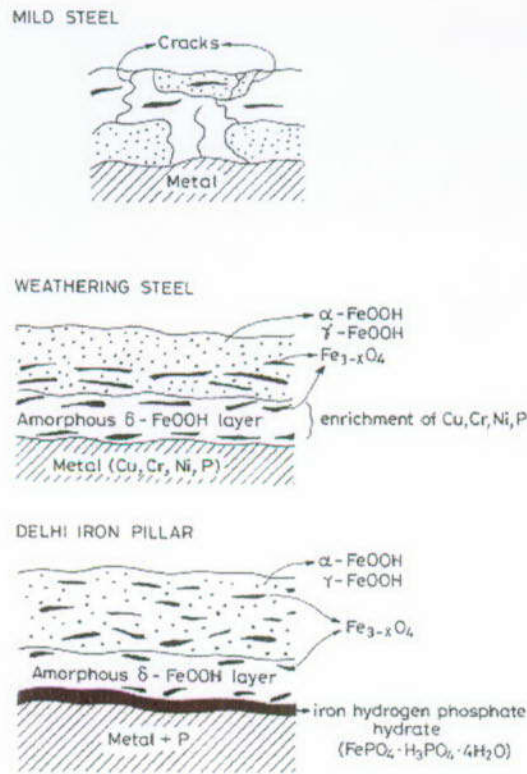
Source: Walton 1994 [127454], Figure 3.

Figure 6-1. Processes Affecting Formation of High-Salinity Fluids on Waste Package Surface



Source: Balasubramaniam 2000 [157383], Figure 1.

Figure 6-2. The Corrosion-Resistant Iron Pillar at Delhi



NOTE: Iron hydrogen phosphate hydrate layer on Delhi iron pillar forms a protective, impermeable coating that retards further corrosion.

Source: Balasubramaniam 2000 [157383], Figure 7.

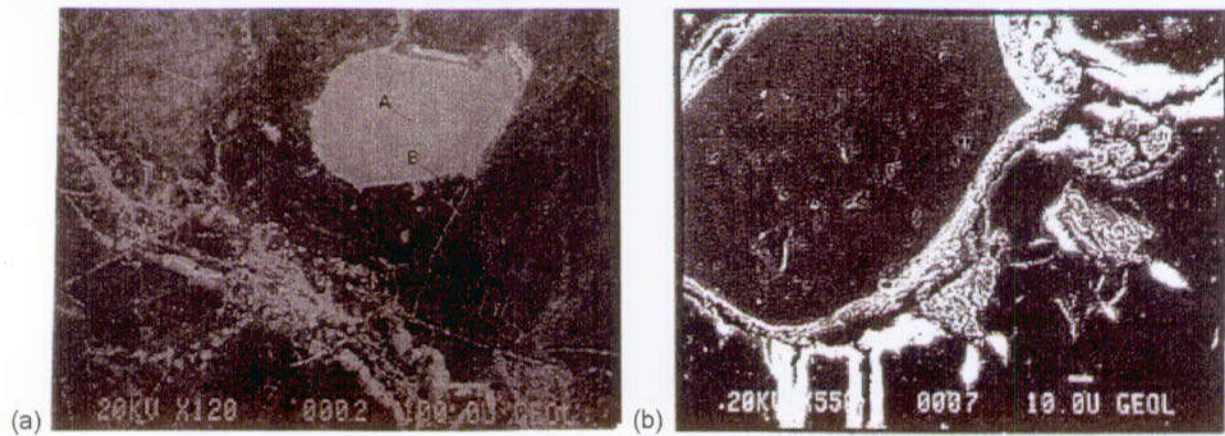
Figure 6-3. Schematic Showing Development of Rust Coating on Mild Steel, Weathering Steel, and Delhi Iron Pillar



NOTE: Metallic-looking areas were analyzed using X-ray photoelectron spectroscopy.

Source: BSC 2001 [157151], Appendix E, Figure 3.

Figure 6-4. Josephinite Sample Used for Surface Analysis Study



NOTE: White rim around chromite in (b) reflects dissolution of exsolution border around chromite.

Source: Robles-Camacho and Armienta 2000 [157386], Figures 5 and 8.

Figure 6-5. Chromite Grains in Serpentine Before (a) and After (b) Acid Leaching

Table 6-1. Composition of Synthetic Yucca Mountain Waters (mg/L) from Unsaturated and Saturated Zones and Their Evaporated Compositions

	Synthetic J-13 water	"157 x" J-13 water	"956 x" J-13 water	Synthetic UZ water	"62 x" UZ water	"1243 x" UZ water
Na	45.2	5,288	43,302	8.56	477	6,223
K	5.2	593	4,701	4.00	268	2,644
Mg	2.1	1.2	0.13	11.8	550	5,546
Ca	5.8	0.06	27.3	57.3	1,713	15,643
SiO ₂	10.4	1,040	----	10.4	503	541
HCO ₃	105	4,410	24,255	20.3	9.9	<45
SO ₄	18.5	2,109	13,209	83.9	1,544	2,098
Cl	7.2	814	5,047	76.6	4,259	52,165
NO ₃	7.9	1,035	5,483	10.7	592	----
F	2.3	237	1,622	2.16	38	<542
TDS	209.6	15,527	97,646	285.7	9,954	~85,000
pH	8.07	10.18	----	7.55	7.65	6-6.5

NOTE: TDS calculated as sum of dissolved solids.

Source: Rosenberg et al. 2001 [154862], Tables 2 and 4.

Table 6-2. Typical Salton Sea Geothermal Well Brine Composition

Component	Concentration ppm	Component	Concentration ppm
Na	49,800	Ba	100
K	12,840	B	301
Mg	80	Cu	7
Ca	24,000	Fe	708
SiO ₂	658	Pb	66
CO ₂	125	Li	177
SO ₄	22	Mn	785
Cl	126,700	Rb	62
NH ₃	339	Sn	402
As	8	Zn	287
I	5	Br	68
pH	5.8	H ₂ S	90
		TDS	261,800

Source: Pye et al. 1989 [157385], Table 1.

7. ENGINEERED BARRIER SYSTEM ANALOGUES

7.1 INTRODUCTION

This section describes the use of natural analogues to evaluate the long-term performance of materials used in the construction of the Engineered Barrier System (EBS) and how these materials may affect radionuclide transport. The primary functions of the EBS components are to: (1) protect the waste package from physical and chemical degradation resulting from processes such as seepage, corrosive fluids, and rock fall; and (2) retard any potential transport of radionuclides from the emplacement drift in the event of waste package failure. Key concerns for the EBS materials (described in Section 5) include the possible degradation and corrosion of metals resulting from mechanical stress, hostile physical and chemical environments, and metallurgical factors. Another important performance parameter is the effect of EBS materials on flow and transport of fluids and dissolved solids into and out of the emplacement drifts. Important issues relating to EBS performance include the degradation of materials caused by corrosive fluids, radiation, thermal and physical stresses, and microbial attack, as well as the effects of sorption and colloids on radionuclide transport. A number of analogues were previously discussed in Section 13 of the *Yucca Mountain Site Description* (CRWMS M&O 2000 [151945]); these analogues are briefly summarized below. Additional analogue examples are discussed in more detail in the following subsections.

Three main issues relating to the EBS were discussed in detail in the natural analogues chapter of the *Yucca Mountain Site Description* (CRWMS M&O 2000 [151945], Section 13.3): (1) metal analogues (native metals and archaeological artifacts) in the evaluation of corrosion resistance; (2) cements and alkaline plumes to determine the impact of high pH fluids on EBS materials, surrounding host rock, and radionuclide transport; and (3) the effects of radiolysis on the integrity of waste package materials. A brief summary of earlier work on metal analogues is presented in Section 6 and thus will not be repeated here.

Under the current EBS design, cementitious material is expected to be present in only minor amounts (as grout for rock bolts) in the near-drift environment. The durability of cements over time has been documented by Gallo-Roman cements that are over 1,500 years old (Thomassin and Rassineux 1992 [157439], p. 137). Cementitious mortar from Hadrian's Wall (~1,700 years old) in England (Figure 7-1) has the same calcium silicate hydrate phases found in modern Portland cement, and still possesses excellent strength and stability (Miller et al. 2000 [156684], p. 131). The potential development of hyperalkaline fluids resulting from interaction of water with cementitious material could affect radionuclide transport and reduce the stability of EBS materials. Two areas with hyperalkaline fluids were described in the earlier review of natural analogues (CRWMS M&O 2000 [151945], Section 13.3.6): the Semail ophiolite in Oman, and the Maqarin area in Jordan. Serpentinization reactions in the Semail ultramafic rocks have resulted in the generation of reducing, hyperalkaline (pH = 10–12) Na-Cl-Ca-OH fluids, with associated minerals brucite ($Mg(OH)_2$) and portlandite ($Ca(OH)_2$). The Maqarin analogue site (also discussed in Section 7.3.1) contains a suite of naturally formed cement minerals, including portlandite. High pH (12–13) fluids emanate from these rocks as a result of reaction of groundwater with the cement phases. These analogue sites have been used in the development of

numerical models to predict water-rock reactions and resulting fluid compositions under similar conditions (McKinley et al. 1988 [126077]; Chambers et al. 1998 [157549]).

Chemical decomposition resulting from radiation (radiolysis) was also examined in the *Yucca Mountain Site Description* (CRWMS M&O 2000 [151945], Section 13.3.7). This process was studied at the natural reactor site at Oklo (in Gabon), where high radiation doses were interpreted to have led to radiolysis of water and redox reactions involving the surrounding rocks (Curtis and Gancarz 1983 [124785]). Similar reactions within the waste package assembly could lead to decomposition of the waste packages and release of radionuclides. However, since the waste loads are configured so that they will not approach criticality and the waste package design excludes free water, the amount of radiolysis that might occur at the potential Yucca Mountain repository should be much less than Oklo (see also Section 4 of this report). Section 7.2 describes analogues for EBS materials and Section 7.3 describes analogues for EBS processes.

7.2 ANALOGUES FOR EBS MATERIALS

7.2.1 Analogues for the Titanium Drip Shield

Corrosion caused by saline fluids has been identified as a potential hazard to the integrity of waste packages (see Section 6.2.1 for discussion). The drip shield assembly is designed to protect the waste packages from physical and chemical degradation resulting from events such as rock falls, seepage, and saline fluids. The current drip shield design calls for corrosion-resistant titanium. Titanium metal does not occur in nature, nor in the archaeological record, so other proxies need to be used to assess its long-term resistance to corrosion.

The Salton Sea geothermal field in California is characterized by hypersaline (15-30 wt% TDS) brines that have caused significant corrosion and scaling problems (Pye et al. 1989 [157385], p. 259). A series of corrosion tests led field operators to select Beta-C titanium (Ti-3Al-8V-6Cr-4Mo-4Zr) for the fabrication of corrosion-resistant production casing (Pye et al. 1989 [157385]). Four tests were conducted over a period from 256 to 833 days, involving installation of full-size Beta-C titanium tubulars in geothermal production wells, resulting in no visible pitting corrosion in two of the tests, little or no change in hydrogen content, and no significant degradation in mechanical properties (Pye et al. 1989 [157385], pp. 262-263). In the 833-day test, localized corrosion was observed, occurring at a rate of 7 mils/yr (178 $\mu\text{m}/\text{yr}$); this was interpreted to have occurred in an area where surface contamination had not been completely removed at the start of the test. Local corrosion was observed along 2 of the 48 casing joints in the fourth test; this corrosion was also interpreted to be the result of pre-existing surface contamination.

A longer-term evaluation of the corrosion behavior of titanium-bearing materials can be obtained by examining the stability of naturally occurring titanium minerals. Titanium is present as a major constituent in a number of refractory accessory minerals commonly found as a minor phase in igneous rocks and in heavy mineral concentrates in sediments. These minerals include sphene (titanite) ($\text{CaTiSiO}_4(\text{O},\text{OH},\text{F})$), rutile (TiO_2), ulvöspinel (Fe_2TiO_4) and ilmenite (FeTiO_3). The Canadian nuclear waste disposal concept includes a metallic titanium container surrounding spent fuel. The corrosion resistance of titanium arises from its passivation in aqueous solutions

by the formation of a protective layer containing rutile (Cramer 1994 [157537], pp. 8–10). At the Cigar Lake uranium deposit in Saskatchewan, Canada, rutile is present within the uranium ore and has persisted unchanged for over a billion years in reducing groundwaters, under hydrothermal conditions, and in a radiation field. While rutile and other titanium-bearing minerals are oxides, and thus do not share the same physical properties as metals, their general resistance to alteration reflects the stable nature of titanium-bearing materials.

7.2.2 Analogues for the Invert Ballast

The nonwelded Calico Hills Formation and portions of the Paintbrush Tuff at Yucca Mountain are possible analogues for processes, such as sorption and ion exchange, that would affect the transport of radionuclides within the crushed tuff invert ballast. The relative lack of fractures in these tuffs results in fluid flow occurring in the tuff matrix, resulting in overall slower fluid flow and transport in these units caused by the lack of fast flow pathways, similar to what is predicted for the crushed tuff invert. Because of the presence of zeolites and/or smectite in the nonwelded tuffs, extensive ion exchange occurs between pore waters and the tuffs (Vaniman et al. 2001 [157427]). The zeolitic tuffs are significantly enriched in cations such as Ca^{2+} , Mg^{2+} , and Sr^{2+} , and depleted in Na^+ and K^+ (Figure 7-2); thus, waters are interpreted to have complementary (opposite) enrichments and depletions (Vaniman et al. 2001 [157427], pp. 3420–3423). This ion-exchange process would have a major impact on radionuclide transport, with species such as ^{90}Sr being effectively immobilized by this process. However, the current design for the invert ballast (DOE 2001 [153849], Section 2.4.1.2) uses crushed tuff derived from the repository interval (welded, devitrified Topopah Spring Tuff), which has only minor amounts of zeolites and clays (Vaniman et al. 2001 [157427], Figure 2). As a result, the ion exchange and sorption capacity of the crushed tuff invert ballast should be significantly lower than that observed in the nonwelded tuffs at Yucca Mountain. The crushed tuff invert would have high effective grain surface areas, which would favor sorption of species onto mineral surfaces, thus serving to retard radionuclide transport.

The effects of fluid flow on radionuclide retardation in ash flow tuff can also be evaluated through an anthropogenic analogue. At Los Alamos National Laboratory, radionuclide-bearing liquid wastes were discharged from 1945 to 1967 into gravel- and cobble-filled absorption beds (approximately 6 m × 37 m) built on outcrops of moderately welded rhyolite ash flow tuff (Figure 7-3) (Nyhan et al. 1985 [157447], p. 502). Large amounts (corresponding to a depth of 20.5 m) of tap water and radioactive effluent were added to one of the absorption beds (Bed 1) in 1961 to evaluate radionuclide mobility. The site was revisited in 1978, when profiles of Pu and ^{241}Am were measured in a series of 30.5 m deep boreholes drilled through two of the absorption beds (Bed 1 and Bed 2) and into the underlying ash flow tuff (Nyhan et al. 1985 [157447], p. 502). This study revealed that the bed where water and effluent had been added in 1961 (Bed 1) exhibited higher water saturations, along with significantly more radionuclide migration out of the absorption bed and into the underlying tuff (Figure 7-4), than the bed where no additional fluid had been added during this test (Bed 2). Plutonium and ^{241}Am were not detected beyond 11.28 m below the bottom of Bed 2, whereas 0.3 to 5.1% of the plutonium and 3.0 to 49% of the americium inventory were present within the depth interval of 11.28–27.13 m for Bed 1 (Nyhan et al. 1985 [157447]), p. 506). Elevated concentrations of radionuclides were observed to occur within lower permeability intervals of the tuff. The radionuclide concentrations of fracture fillings were similar to those of adjacent tuff samples, suggesting that fractures did not enhance

radionuclide transport under unsaturated conditions and generally acted as barriers to unsaturated zone (UZ) flow (Nyhan et al. 1985 [157447], pp. 504–505, 508). These results suggest that radionuclide mobility was triggered by flushing of the absorption beds with large volumes of fluids. The volume of the column of fluid used in the Los Alamos test is equivalent to the amount of percolating surface water expected to flow through Yucca Mountain over a timespan of 2,000 to 4,000 years (assuming an infiltration rate of 5 to 10 mm/yr (Flint et al. 2001 [156351], p. 26), and thus represents an illustration of the effects of flushing on radionuclide mobility. However, this example does suggest that the ability of the invert ballast at Yucca Mountain (as well as the underlying welded tuffs) to retard radionuclide migration will depend in part on the amount of water flowing through this interval. Both of the analogue examples described are also relevant to processes controlling radionuclide transport in the UZ at Yucca Mountain (see Section 9).

7.3 NATURAL ANALOGUES FOR EBS PROCESSES

The physical and chemical conditions for the near-field area around the emplacement drifts at Yucca Mountain are predicted to undergo changes over time. These changes would result from coupled thermal-hydrologic-chemical (THC) processes, such as boiling, condensation, fluid flow and transport, and mineral dissolution, alteration, and precipitation (BSC 2001 [154677]). THC processes are also expected to occur within the EBS, and could lead to degradation of the EBS components, resulting in the release and transport of radionuclides away from the EBS. Natural analogue studies for some of the processes expected to impact the EBS system, such as the generation of alkaline plumes resulting from interaction of water with cementitious material and the effects of colloids on radionuclide transport, are described below.

7.3.1 Natural Analogues for Development of Alkaline Plumes from Cement

The presence of naturally occurring cement minerals and associated hyperalkaline groundwaters at Maqarin, Jordan, has been used as a natural analogue for examining the effects of hyperalkaline waters (e.g., Khoury et al. 1992 [125677]; Smellie 1998 [126633]). The Maqarin site consists of interbedded bituminous limestones and marls that have been locally thermally metamorphosed from spontaneous combustion of the bitumen, resulting in the calcination of limestone and formation of cement minerals, including portlandite. Water interacting with portlandite has resulted in the formation of highly alkaline (pH \approx 12.5) groundwaters and the precipitation of minerals such as ettringite and thaumasite at ambient temperatures (Figure 7-5). Initial geochemical modeling efforts resulted in model predictions of dissolved selenium and uranium concentrations that were several orders of magnitude higher than those observed in the field (Linklater et al. 1996 [108896], p. 67). A multicomponent reactive transport model that incorporated mixed equilibrium and kinetic reactions was applied to simulate rock alteration mineralogy and fluid chemistry changes for discrete fractures in the Maqarin system (Steeffel and Lichtner 1998 [156714]). These simulations predict the formation of hydrated calcium sulfate and silicate minerals, such as ettringite and tobermorite, which were observed in the field (Khoury et al. 1992 [125677], p. 122), and also reproduced measured fluid pH values. The simulations suggest that mineralization caused by interaction of the hyperalkaline plume with surrounding rocks may result in both reduction of matrix porosity and fracture sealing. Fractures at the Maqarin site have complex mineralogy and textures that suggest that they have undergone repeated sealing and reopening over time. The relative rates of matrix and fracture mineralization

(and associated reduction in permeability) will significantly affect the mobility of the alkaline plume, and thus the transport of associated radionuclides.

The development of large hyperalkaline plumes and associated alteration and transport are not expected to occur at Yucca Mountain. The amount of cementitious material expected to be present in the potential repository (in the form of grout around rock bolts in the emplacement drifts) is much less than what is observed at Maqarin. The fluid pH of the near-field environment thus will be buffered by tuff rather than by portlandite, resulting in less alkaline pH conditions (DOE 2001 [153849], Section 4.2.3.3.3). The Maqarin natural analogue is important to consider in illustrating the effects of alkaline fluids on water-rock processes, and thus constraining EBS design parameters (through minimization of the use of cement) and coupled process models. The ability of the multicomponent reactive transport simulations to reproduce observed water-rock interactions for the alkaline plumes at Maqarin provides confidence that similar THC modeling efforts at Yucca Mountain predict reactive chemistry and transport processes that are expected to occur over time.

7.3.2 Natural Analogues for Colloidal Transport of Radionuclides

Colloids can facilitate radionuclide transport (Figure 7-6) if they are: (1) present in sufficient quantities, (2) mobile, and (3) can bind radionuclides (Wieland and Spieler 2001 [157442], p. 511). Naturally occurring colloids are ubiquitous in groundwaters; sampled by Kingston and Whitbeck (1991 [113930], pp. 26, 57) (mainly from central and southern Nevada) have dilute colloid concentrations ranging from 0.28–1.35 mg/L, and ferric oxide and oxyhydroxide colloids can also be generated through degradation of structural steel present in EBS materials.

Filtration of Fe-bearing colloids has been documented in some environments. For instance, groundwaters in the Poços de Caldas area, Brazil, typically have low concentrations (<1 mg/L) of colloids (Miekeley et al. 1989 [126083], pp. 838, 840–841; 1991 [127199], pp. 35, 49). Most of the colloids there are composed of iron and organic species. Only minor amounts of uranium are associated with colloids, but greater amounts of thorium and rare earth elements are transported in the colloidal fraction. The results of the colloid studies at Poços de Caldas (Miekeley et al. 1989 [126083], p. 841; 1991 [127199], p. 58) suggest that radionuclide and other trace-element transport by colloids does not play a significant role in the geochemical processes of weathering, dissolution, and erosion of these ore deposits. One reason for this could be filtration of material which traps colloids in pore throats and narrow fractures (Smellie et al. 1989 [126636], p. 868). The colloidal material acts as an efficient and largely irreversible sink or trap for many elements (especially if they are immobile), but needs to be taken into account in equilibrium thermodynamic modeling of radionuclide speciation. The point of this example is that the iron-bearing colloids that may form in the Exploratory Studies Facility could be beneficial in complexing with uranium and could be retained effectively in the EBS by filtration.

7.4 SUMMARY

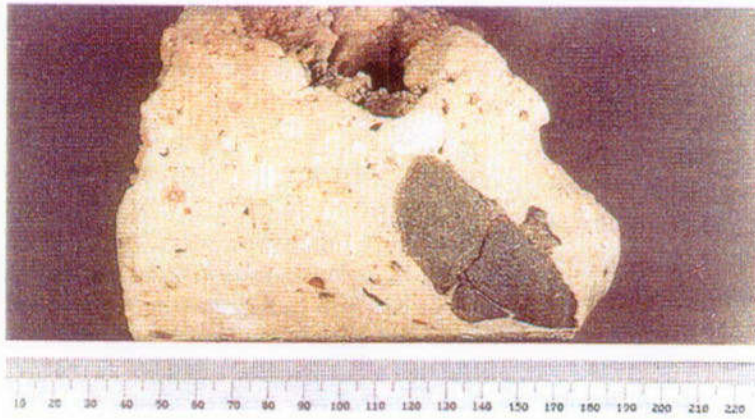
The highly corrosive-resistant nature of titanium has been demonstrated by long-term experiments conducted on a range of metal alloys in wells at the Salton Sea geothermal field. The commercial use of titanium alloys in production casings over the past decade at the Salton Sea has greatly alleviated severe corrosion problems that were previously experienced resulting

from exposure of conventional steel casing to the hot, hypersaline geothermal brines. This anthropogenic example supports the selection of titanium alloys for the construction of a corrosion-resistant drip shield for the EBS.

Mineralogic and geochemical analysis of tuffs in the UZ at Yucca Mountain indicates that the presence of zeolite and clay minerals greatly enhance cation exchange, thus serving to retard the transport of some radionuclides. While the proposed material (devitrified welded tuff) for the invert ballast in the current design does not have high concentrations of these minerals, the high surface area of crushed tuff will retard radionuclide transport through absorption. The Los Alamos example of actinide absorption in a gravel bed provides qualitative evidence of retardation at the contact between an invert-like material and underlying bedrock.

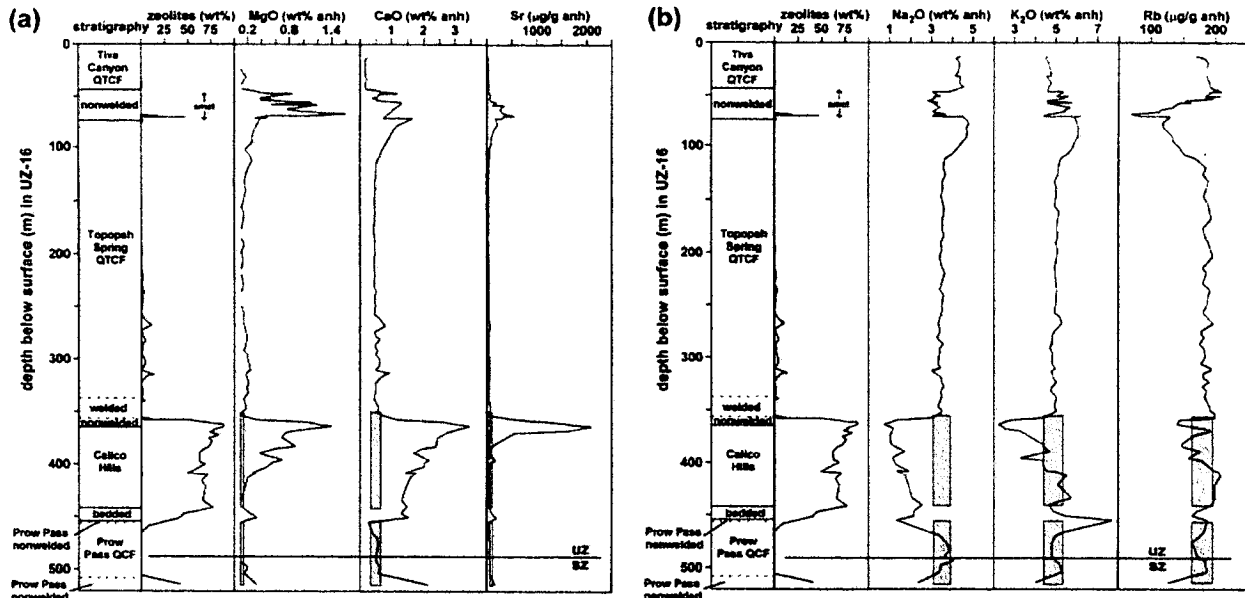
The presence of cementitious materials can potentially lead to the development of alkaline plumes, resulting in corrosion of waste package materials, alteration of surrounding host rocks, and possible enhancement of radionuclide transport. Because the use of cementitious material in the EBS and its environs is restricted to grout for securing rock bolts in the emplacement drifts, hyperalkaline conditions are not expected to develop at Yucca Mountain. However, through reactive transport modeling of the Maqarin site, it has been demonstrated that a model can reproduce the same suite of cement minerals, hyperalkaline water compositions, and pH that were found in the field, thus building confidence in use of such a model for analogous conditions at other sites.

The Poços de Caldas analogue illustrated that iron-bearing colloids may retard the transport of uranium and other spent-fuel components by forming colloids that are then filtrated from suspension at short distances. Degradation of steel structural elements in the EBS could conceivably contribute to this process.



Source: Miller et al. 2000 [156684], Figure B10.2.

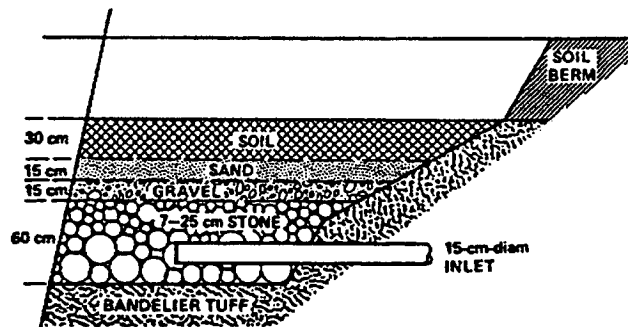
Figure 7-1. Portion of Hadrian's Wall in England, Showing Strength and Stability of Roman Mortar after 1,700 Years



NOTE: Shaded bars represent corresponding compositions of unzeolitized precursor tuffs. Symbols (Q = quartz, T = tridymite, C = cristobalite, F = feldspar) indicate devitrification minerals in welded tuff intervals. UZ-SZ line marks location of water table. Chemical abundances are normalized to anhydrous (anh) compositions.

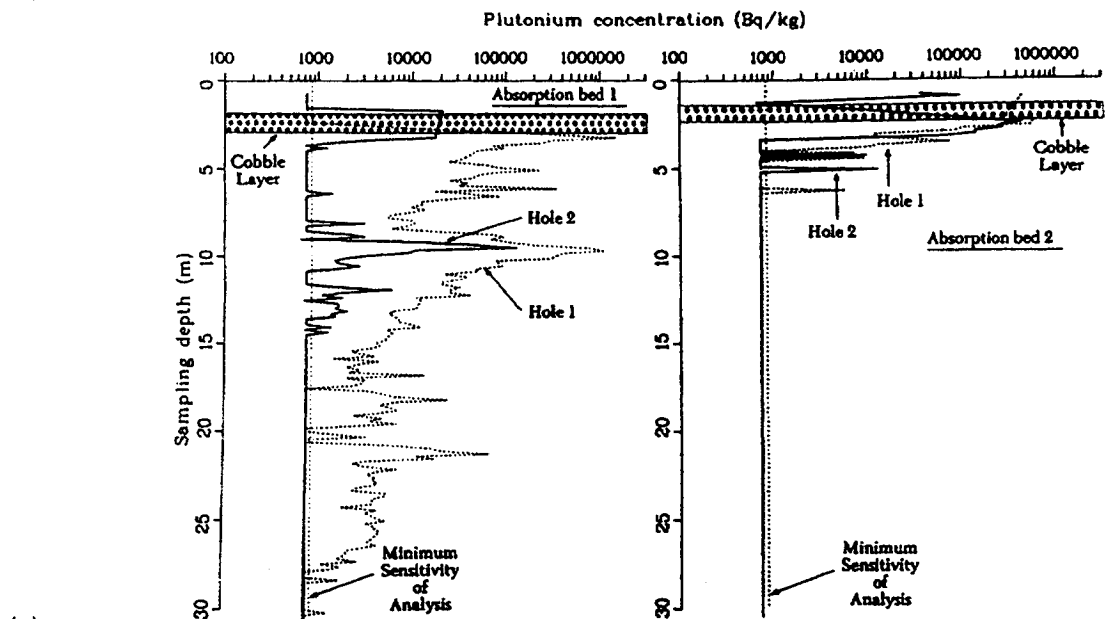
Source: Vaniman et al. 2000 [157427], Figure 4.

Figure 7-2. Stratigraphic Section of Drill Hole UE-25 UZ#16, with Abundance of Zeolites Plotted versus (a) Alkaline Earth and (b) Alkali Constituents

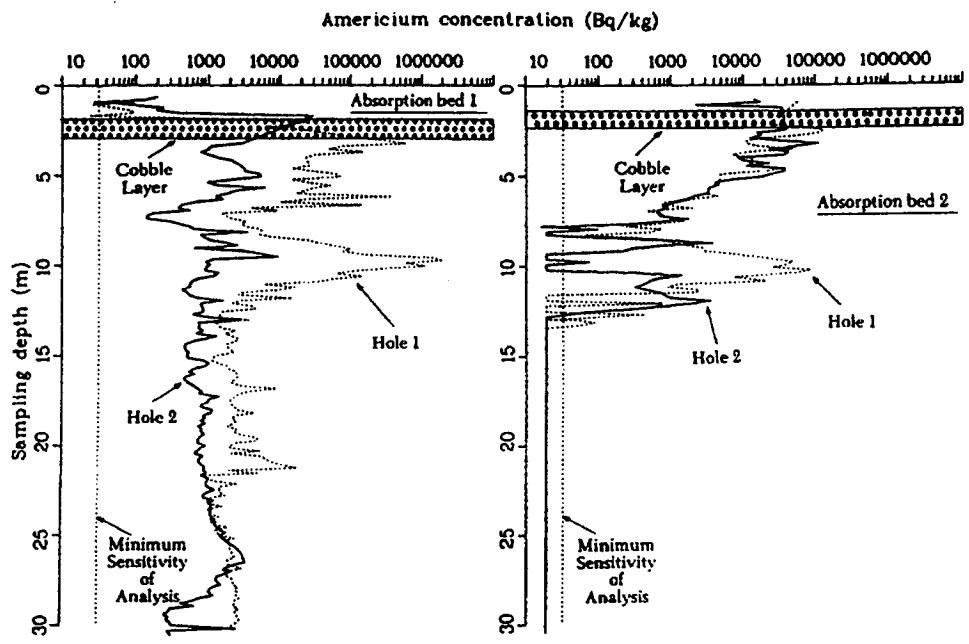


Source: Nyhan et al. 1985 [157447], Figure 1.

Figure 7-3. Cross Section of Absorption Bed for Disposal of Radioactive Liquid Wastes, Area T, DP West Site, Los Alamos National Laboratory



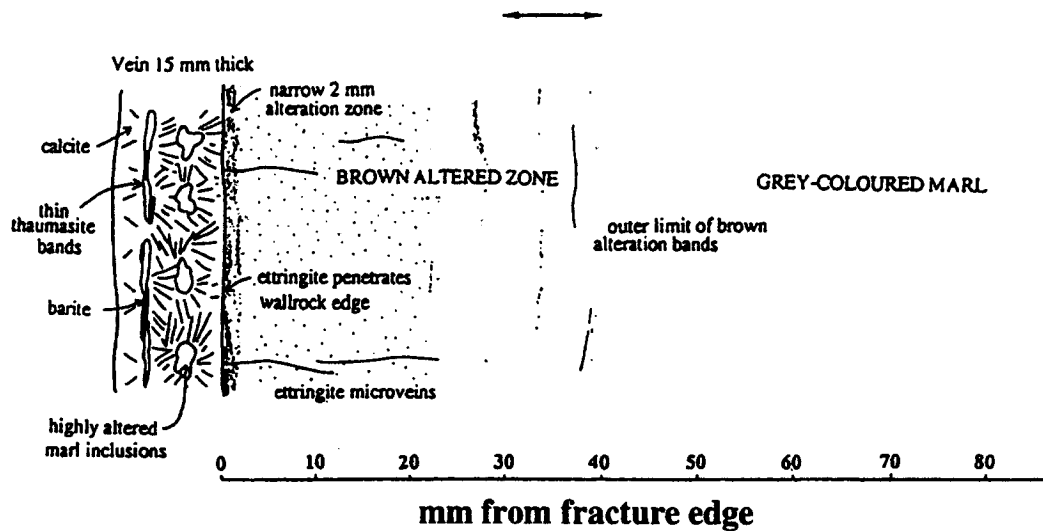
(a)



(b)

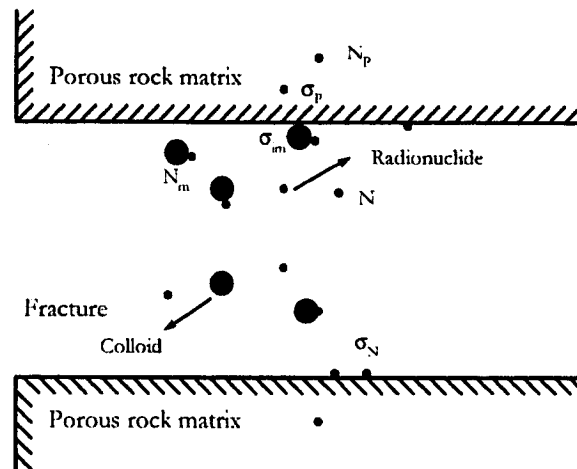
Source: Nyhan et al. 1985 [157447], Figures 2 and 3.

Figure 7-4. Concentrations of Plutonium (a) and Americium-241 (b) within and beneath Absorption Beds 1 and 2, Area T, DP West Site, Los Alamos National Laboratory (1978)



Source: Steefel and Lichtner 1998 [156714], Figure 6.

Figure 7-5. Fracture Mineralization and Wall Rock Alteration at C353 Site, Maqarin, Showing the Presence of Hydrated Calcium Silicate and Sulfate Phases Thaumasite and Etringite



NOTE: N = dissolved radionuclides in fracture,
 σ_N = radionuclides on fracture surface,
 N_m = radionuclides bound to mobile colloids,
 σ_{im} = radionuclides sorbed on immobile colloids,
 N_p = dissolved radionuclides in pores of rock matrix,
 σ_p = radionuclides sorbed on rock matrix.

Source: modified from Jen and Li 2001 [157463], Figure 1.

Figure 7-6. Schematic Illustration of Radionuclide Transport in a Fractured Rock

8. NATURAL ANALOGUES FOR SEEPAGE

8.1 INTRODUCTION

This section examines several different types of qualitative and quantitative natural analogues for seepage, taken from caves, lava tubes, tombs, rock shelters, and buildings that were investigated since publication of the *FY 01 Supplemental Science and Performance Analyses [SSPA], Volume 1: Scientific Bases and Analyses* (BSC 2001 [155950]). It considers the role of the hydrogeologic setting of underground openings on seepage and the effect of relative humidity. It evaluates a number of candidate settings that have been suggested as analogues and demonstrates why they are or are not considered appropriate as seepage analogues. It also examines the question of the preponderance of evidence of preservation of seepage analogues. In this section, the term *infiltration* is used for precipitation that is not lost by runoff, evaporation, or transpiration, and *seepage* is used for that portion of the infiltration within the unsaturated zone (UZ) that enters tunnels or other underground openings. For reference, current precipitation at Yucca Mountain is about 190 mm/yr (DOE 2001 [153849], Section 4.2.1.2.1), with future rates predicted to be 269 to 529 mm/yr (BSC [155950], Table 3.3.1-5). Information found in Sections 8.2, 8.3, and 8.4 may help to support arguments associated with Key Technical Issue (KTI) KUZ0407 found in Table 1-1.

8.2 GEOLOGIC EXAMPLES

Seepage is mainly governed by the capability of individual fractures to hold water by capillary forces, and by the permeability and connectivity of the fracture network, which enables water to be diverted around a drift or underground opening. Both properties determine the effectiveness of the capillary barrier in diverting flow and thus reducing seepage rates below the prevailing percolation flux. Percolation is the downward or lateral flow of water that becomes net infiltration in the UZ. The physical properties of water, together with the hydrologic properties of rock, lead to the prediction that much of the infiltrating water in the UZ will be preferentially diverted around openings, such as tunnels, at the potential mined geologic repository at Yucca Mountain. The percentage of infiltration that can become seepage decreases as infiltration decreases, and at low infiltration rates (<5 mm/yr) and most permeabilities, no seepage occurs (DOE 2001 [153849], Section 4.2.1.4.2). Two natural analogue studies confirm the prediction that most infiltration does not become seepage.

In a two-year study at Kartchner Caverns, Arizona, yearly precipitation ranged from 288 mm to 607 mm, and averaged 448 mm/yr (Buecher 1999 [154295], pp. 108–109). This was similar to the long-term average at two nearby stations. Estimates of seepage into the cave by three methods based on infiltration and precipitation measurements ranged from 4.3 mm/yr to 12.4 mm/yr, with an average of 7.9 mm/yr (Buecher 1999 [154295], p. 110). Thus, less than 2% of the available moisture became seepage. This low seepage occurs even though the cave, which covers an area of approximately 350 m (N-S) by 550 m (E-W), is cut by more than 60 mapped faults (Jagnow 1999 [154296], p. 49 and Figure 3).

The cave at Altamira, Spain, was monitored for 22 months by Villar et al. (1985 [145806]). The volume of water flowing from 9 of 14 “significant drips” was measured, and an average total